

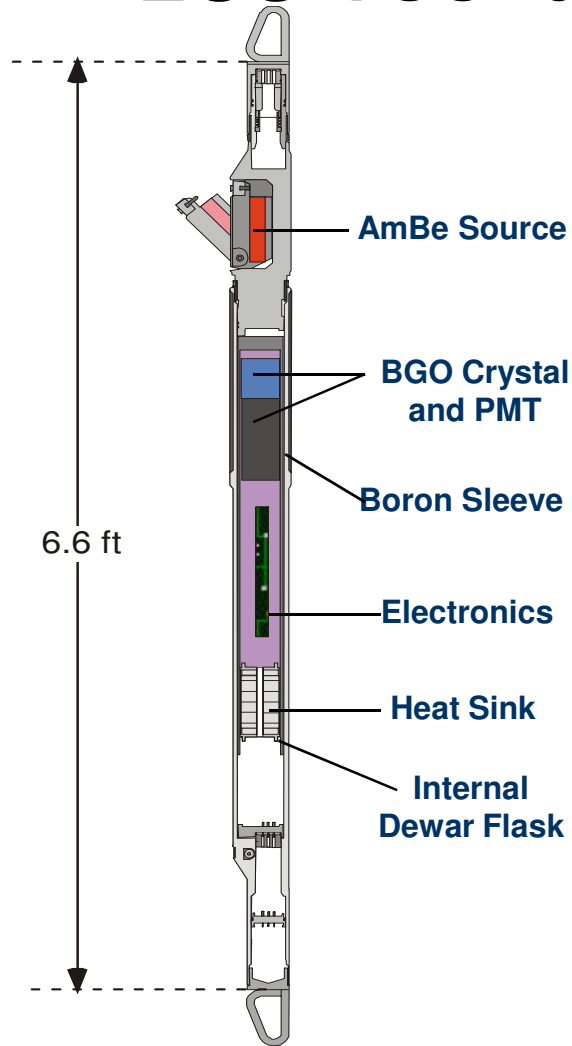
# Borehole Elemental Concentration Logs Now Available: A New Source of Geochemistry Data

Michael Herron, Susan Herron, Jim Grau  
Schlumberger-Doll Research

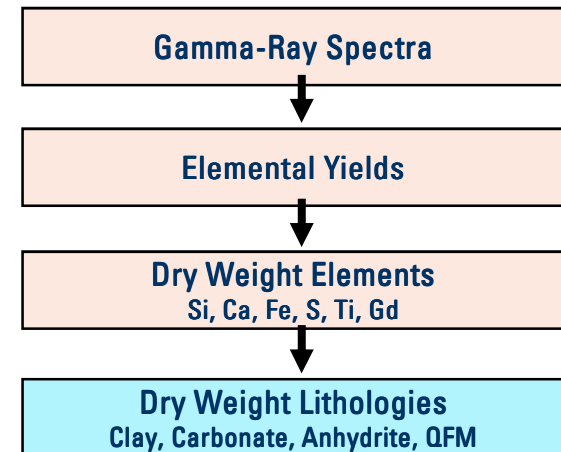
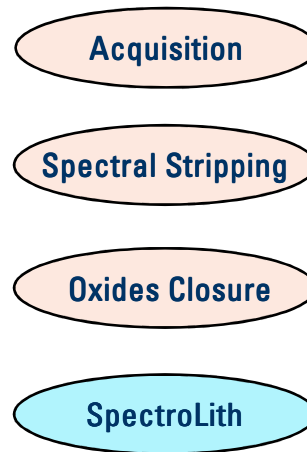
# Leaps of Science Follow New Analytical Capabilities

- Well logging provides more data every day about earth formations than all laboratory sources in a year
- Geochemical well logging is a new analytical capability
- Time for earth scientists to address this new source of data

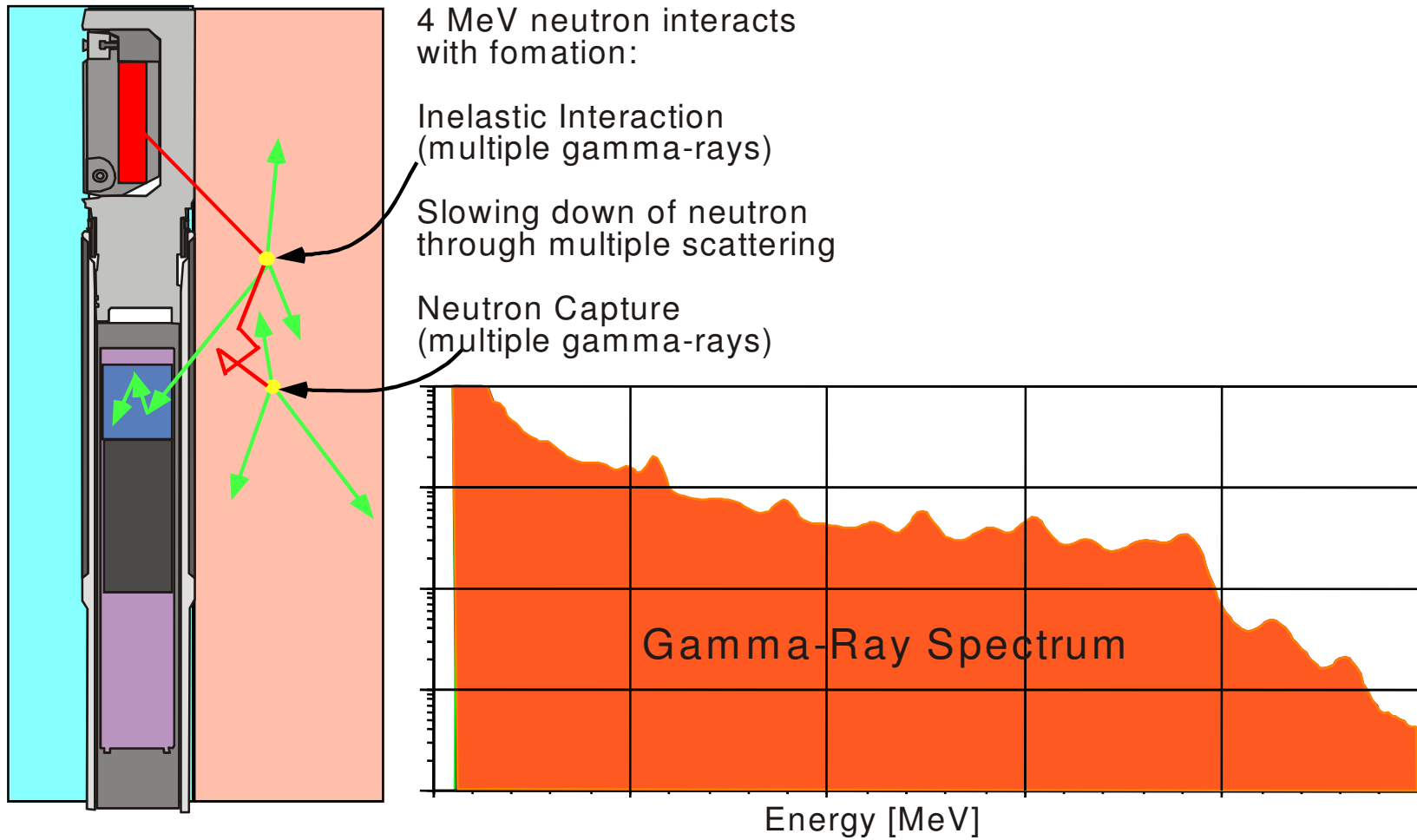
# ECS Tool and Data Processing Flow



- Logging Speed: 1800 ft/hr
- Vertical Resolution: 1.5 ft
- Borehole Fluid: All
- Tool Size: 5.0 in O. D.
- Length: 6.6 ft
- Maximum Temp: 350 °F
- Maximum Pressure: 20,000 psi
- Min Hole Size: 6.00 in

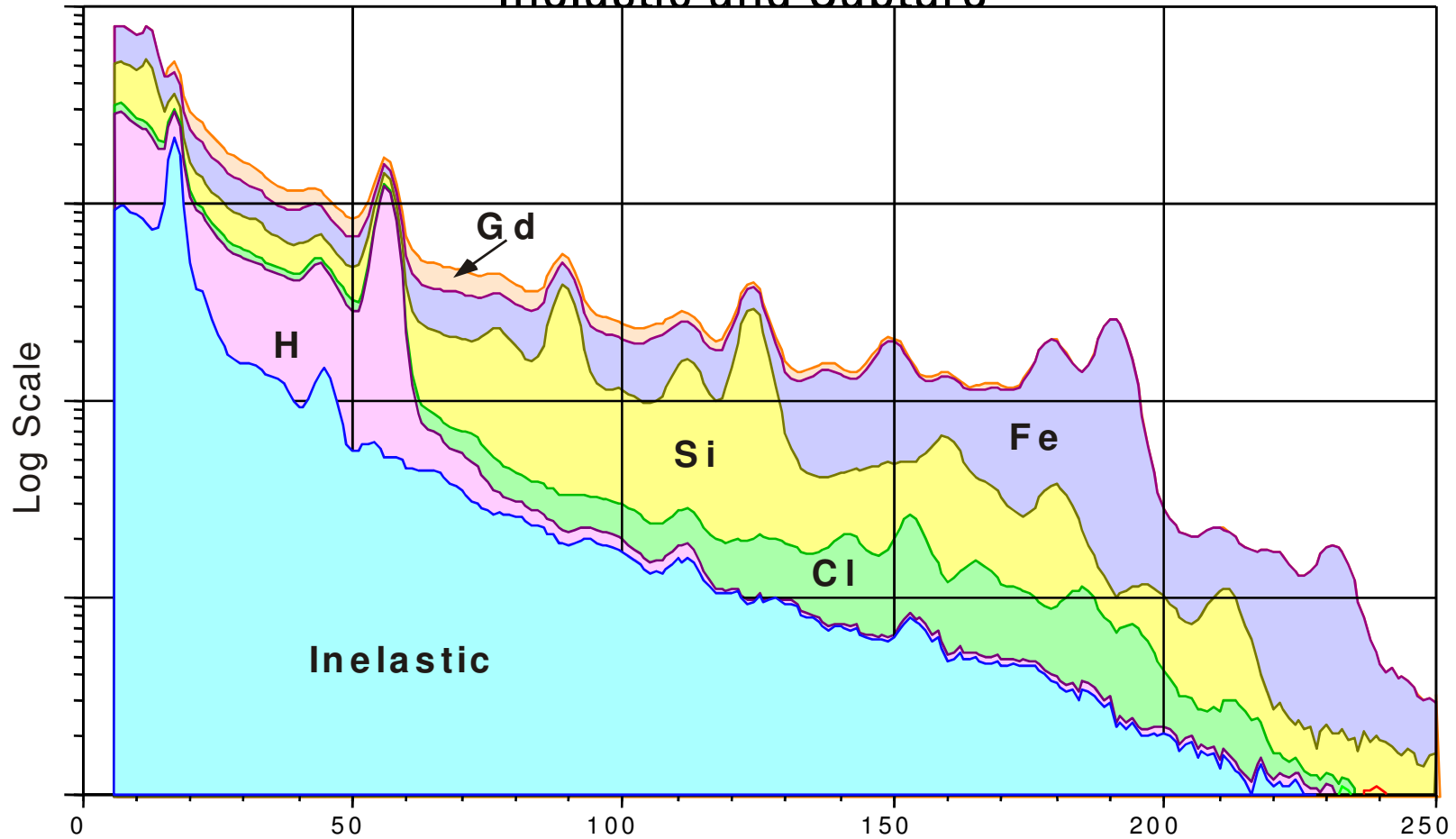


# What Do We Measure ?

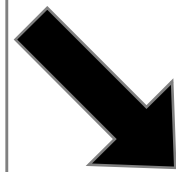
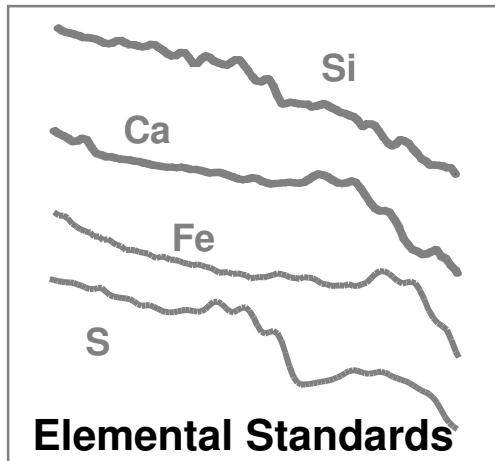
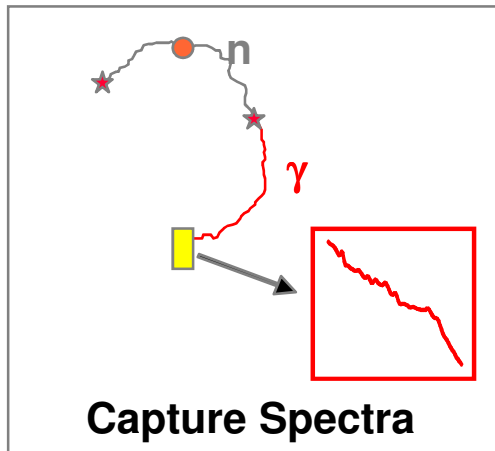


# ECS Gamma-Ray Spectrum

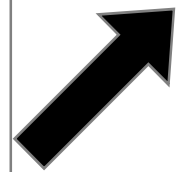
Inelastic and Capture



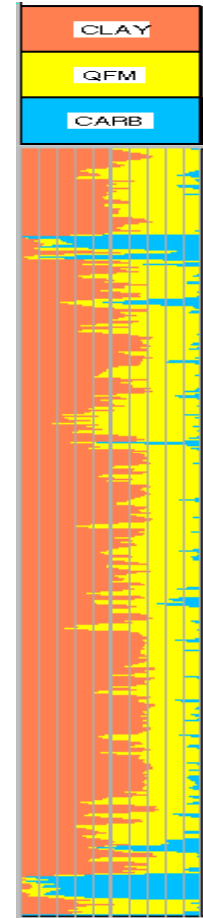
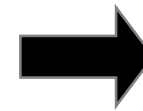
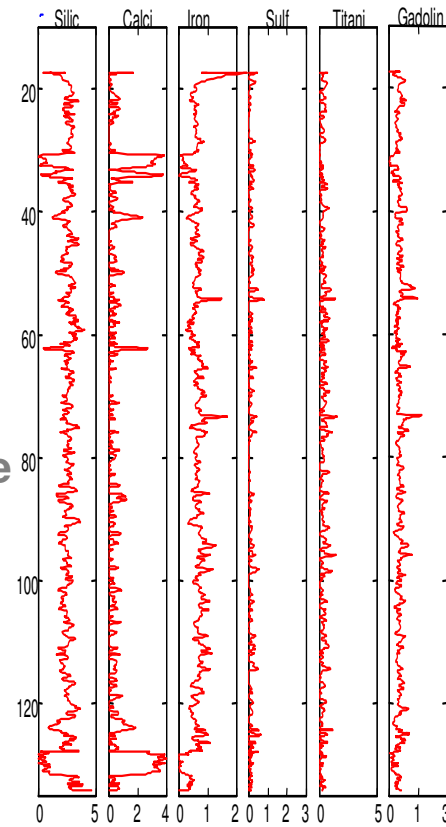
# Capture Gamma-Ray Spectroscopy



Relative  
Yields



Oxides  
Closure

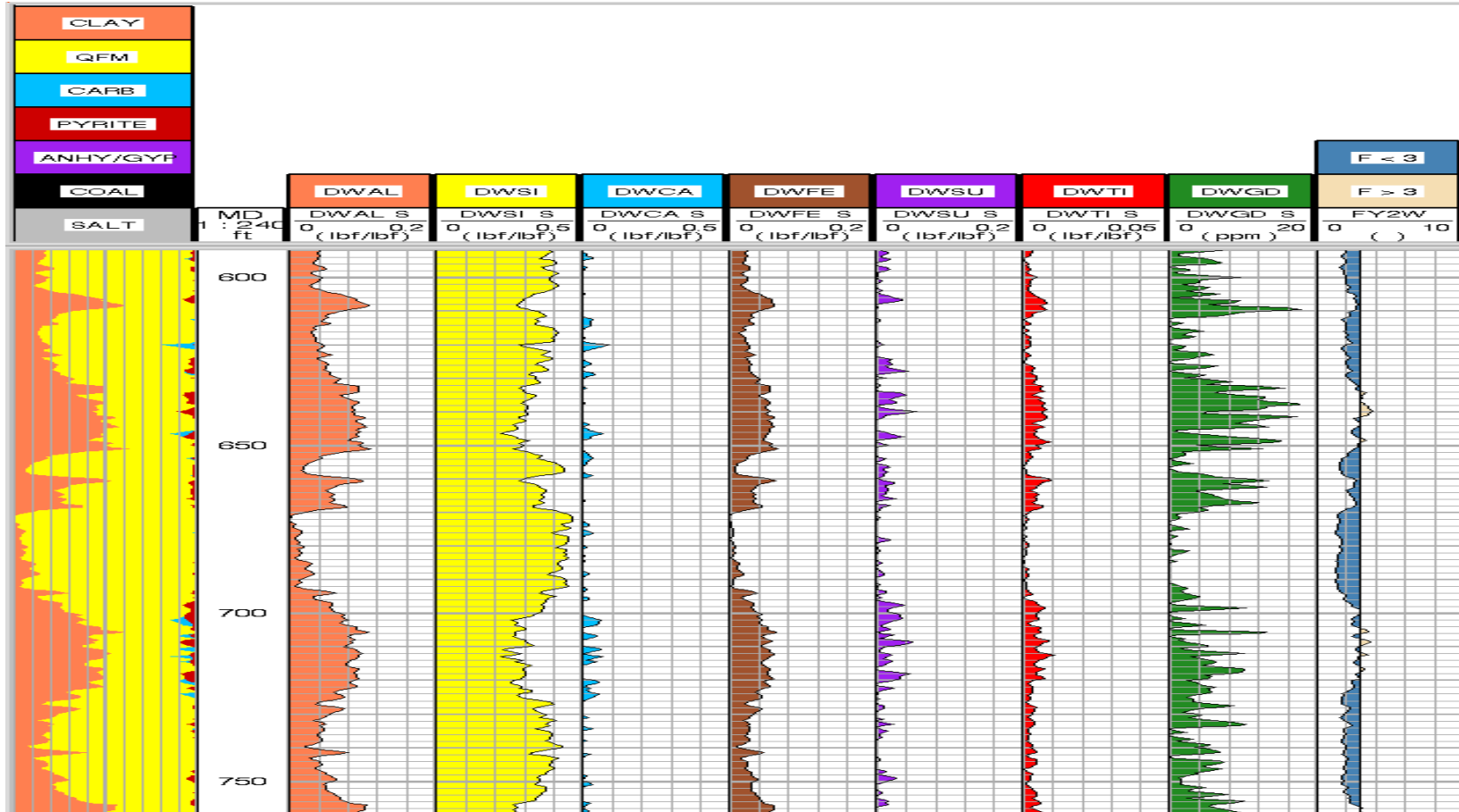


**Elemental Concentrations**

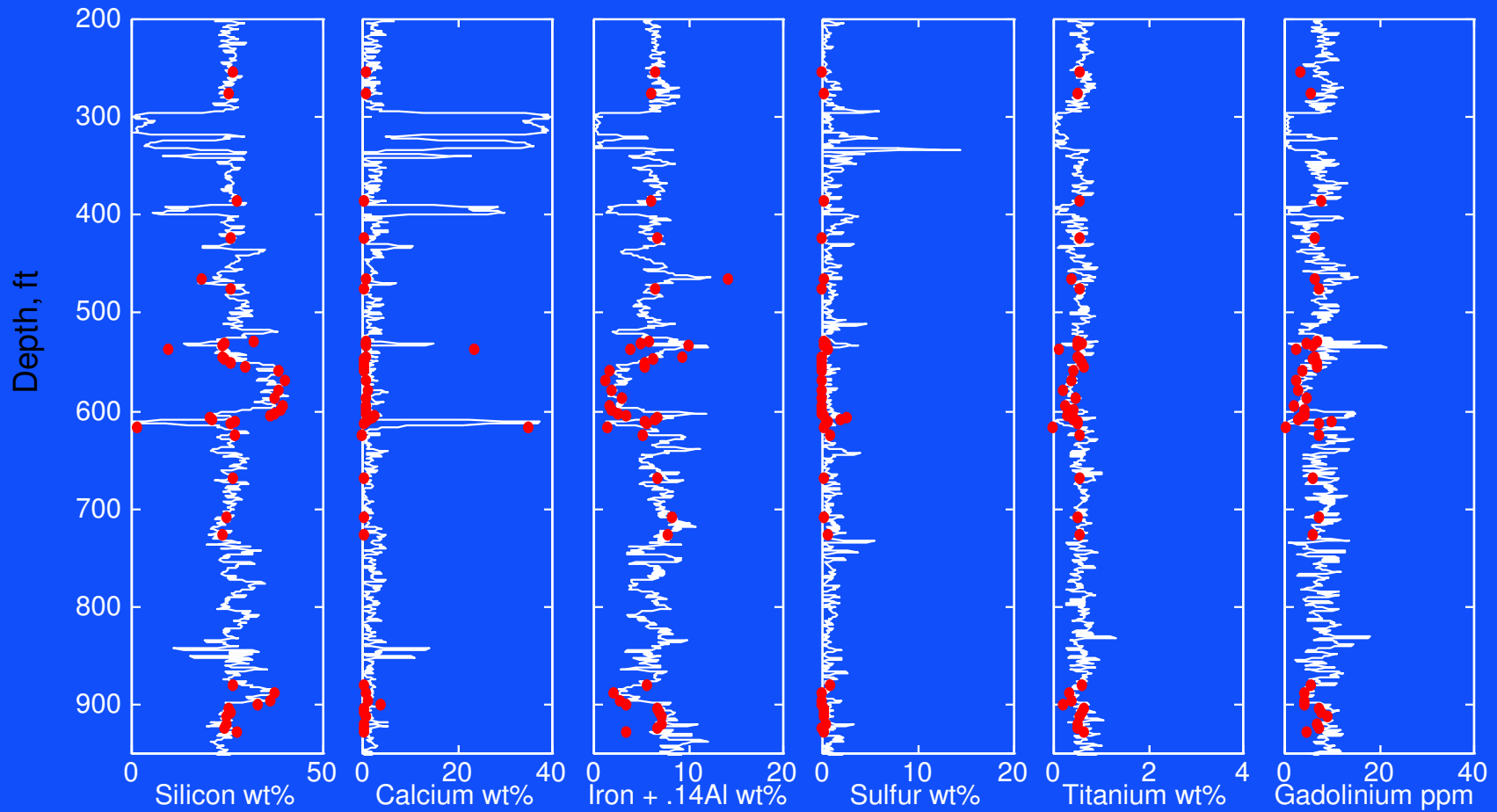
**Lithology**

# ECS SpectroLith

## Dry Weight Lithologies and Elements

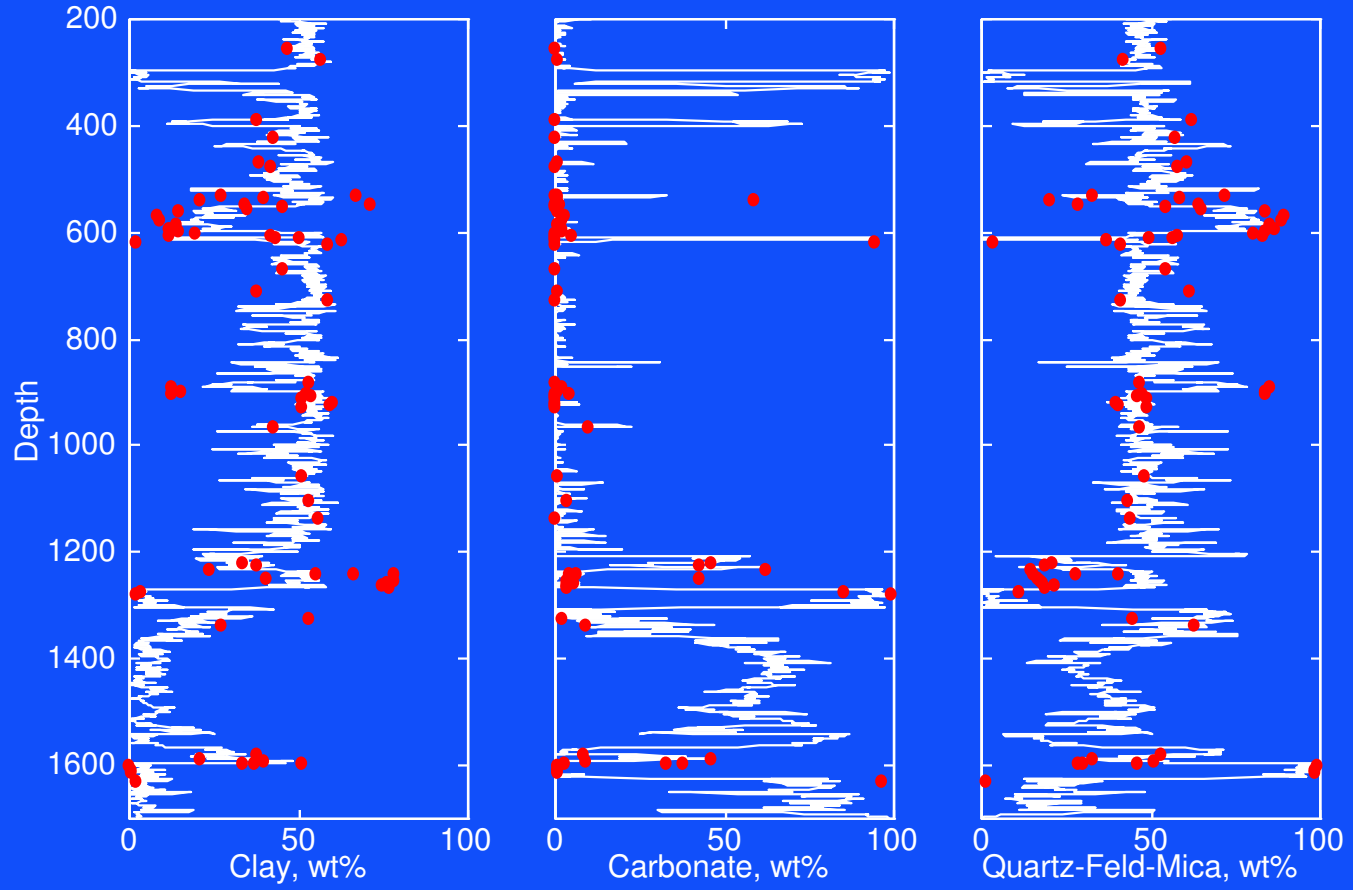


# Open Hole Elemental Concentrations





# Open Hole Lithology



# Instant Petrophysical Evaluation

Nuclear spectroscopy  
SLB exclusive hardware  
and interpretation

+

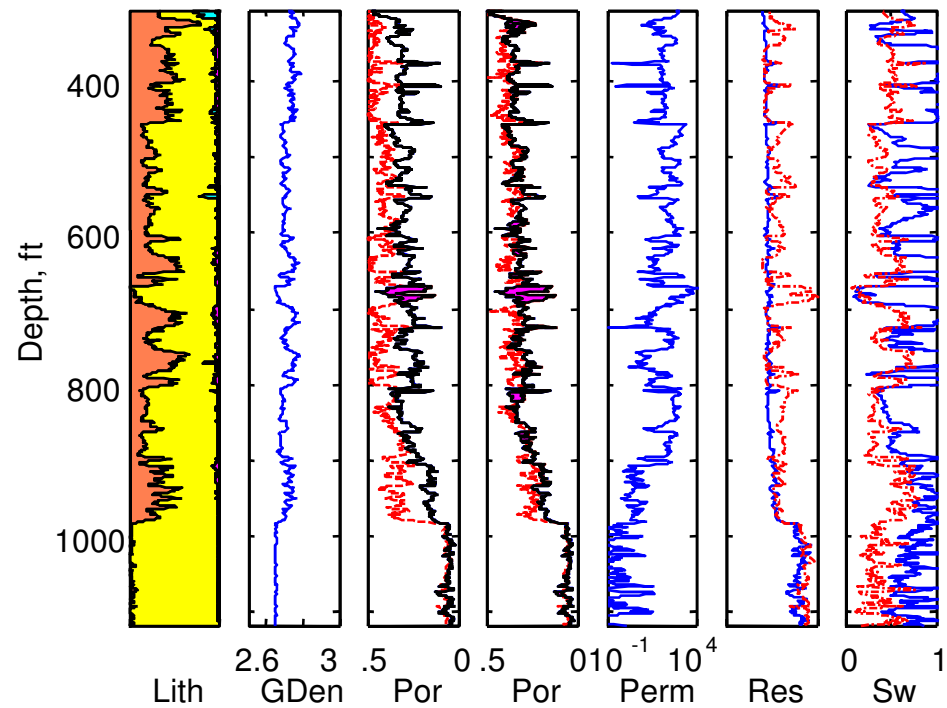
Triple Combo

=

Real-Time Petrophysics

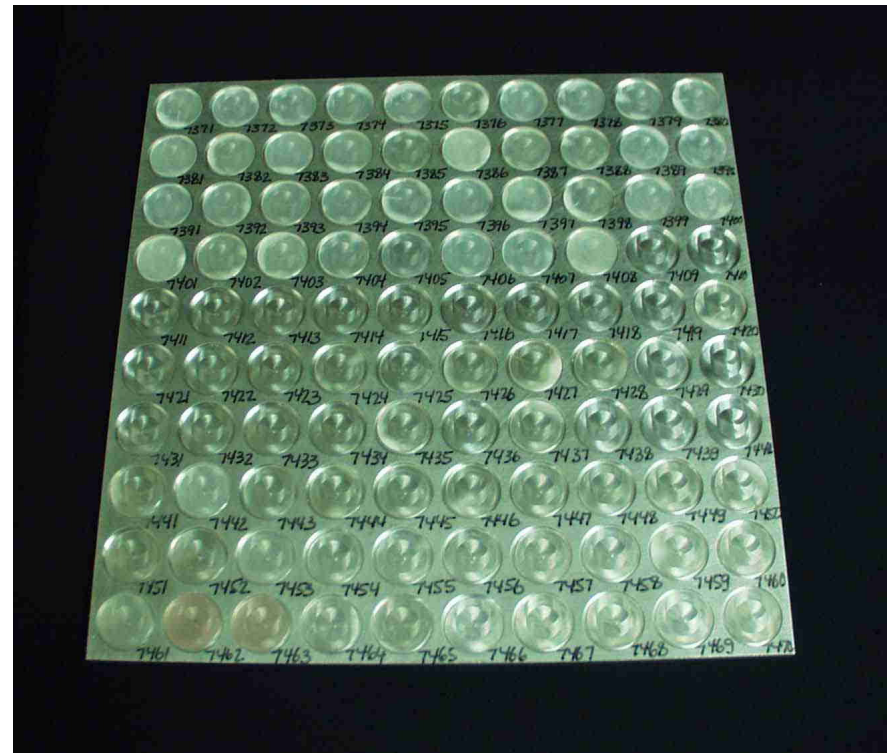
Wireline & LWD

*Siliciclastics – Four patented applications*



# SDR Fourier Transform Infrared Spectroscopy Quantitative Mineralogy

- Recognized world-class
- Patented
- Best paper 1997 Society of Core Analysts



# Commercial XRD and Actual Mineralogy

Sample A	Qtz	Ksp	Plag	Cal	Mg-Cal	Dol	Sid	Py	Kaol	2:1 Al clay	2:1 Fe clay	Fe-Chl
Actual	25	5	5	5	0	0	0	0	15	20	20	5
Vendor 1	68	3	4	5	0	0	0	0	8	11		0
Vendor 2	44	1	5	2	0.1	0	0.1		23	12		11
Vendor 3	41	2	3	9	0	0	0	0	36	9		0
Sample B	Qtz	Ksp	Plag	Cal	Mg-Cal	Dol	Sid	Py	Kaol	2:1 Al clay	2:1 Fe clay	Fe-Chl
Actual	30	5	10	5	0	5	0	5	20	10	0	10
Vendor 1	56	0	7	3	0	6	0	14	12	2		1
Vendor 2	34	1	8	3	0	6	0	4	24	2		18
Vendor 3	52	2	3	13	0	0	0	2	24	5		0
Sample C	Qtz	Ksp	Plag	Cal	Mg-Cal	Dol	Sid	Py	Kaol	2:1 Al clay	2:1 Fe clay	Fe-Chl
Actual	30	10	5	5	5	5	10	0	10	15	0	5
Vendor 1	63	3	14	3	0	5	6	0	5	1		0
Vendor 2	39	2	6	4	0	7	14	0.2	15	4		10
Vendor 3	37	1	2	8	0	9	19	0	19	5		0

D. McCarty (Chevron)

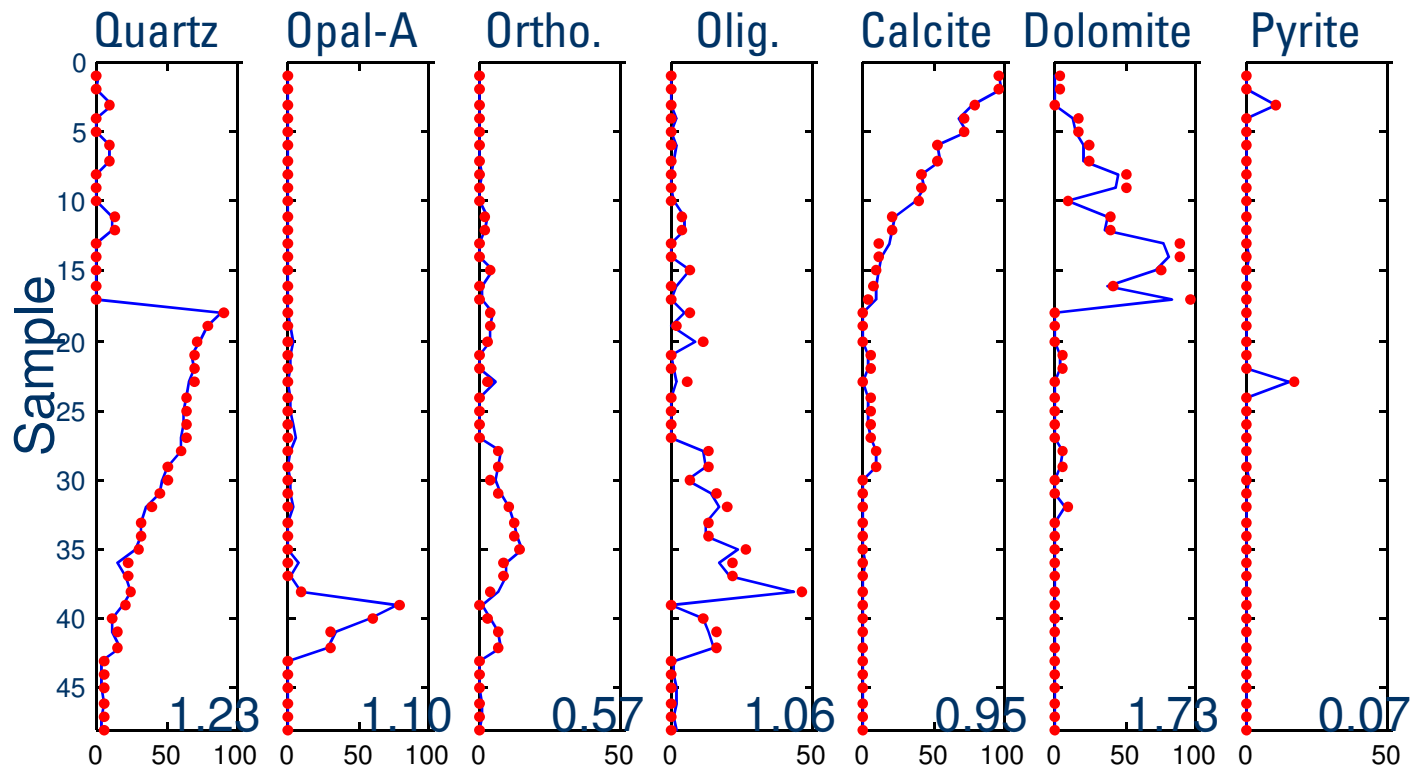
# Commercial XRD and Actual Mineralogy

<b>Sample A</b>	<b>Qtz</b>
<b>Actual</b>	<b>25</b>
<b>Vendor 1</b>	<b>68</b>
<b>Vendor 2</b>	<b>44</b>
<b>Vendor 3</b>	<b>41</b>
<b>Sample B</b>	<b>Qtz</b>
<b>Actual</b>	<b>30</b>
<b>Vendor 1</b>	<b>56</b>
<b>Vendor 2</b>	<b>34</b>
<b>Vendor 3</b>	<b>52</b>
<b>Sample C</b>	<b>Qtz</b>
<b>Actual</b>	<b>30</b>
<b>Vendor 1</b>	<b>63</b>
<b>Vendor 2</b>	<b>39</b>
<b>Vendor 3</b>	<b>37</b>

D. McCarty (Chevron)

# True and Estimated Mineral Concentrations

True Composition  
Estimated from FT-IR



# True and Estimated Mineral Concentrations

True Composition  
Estimated from FT-IR

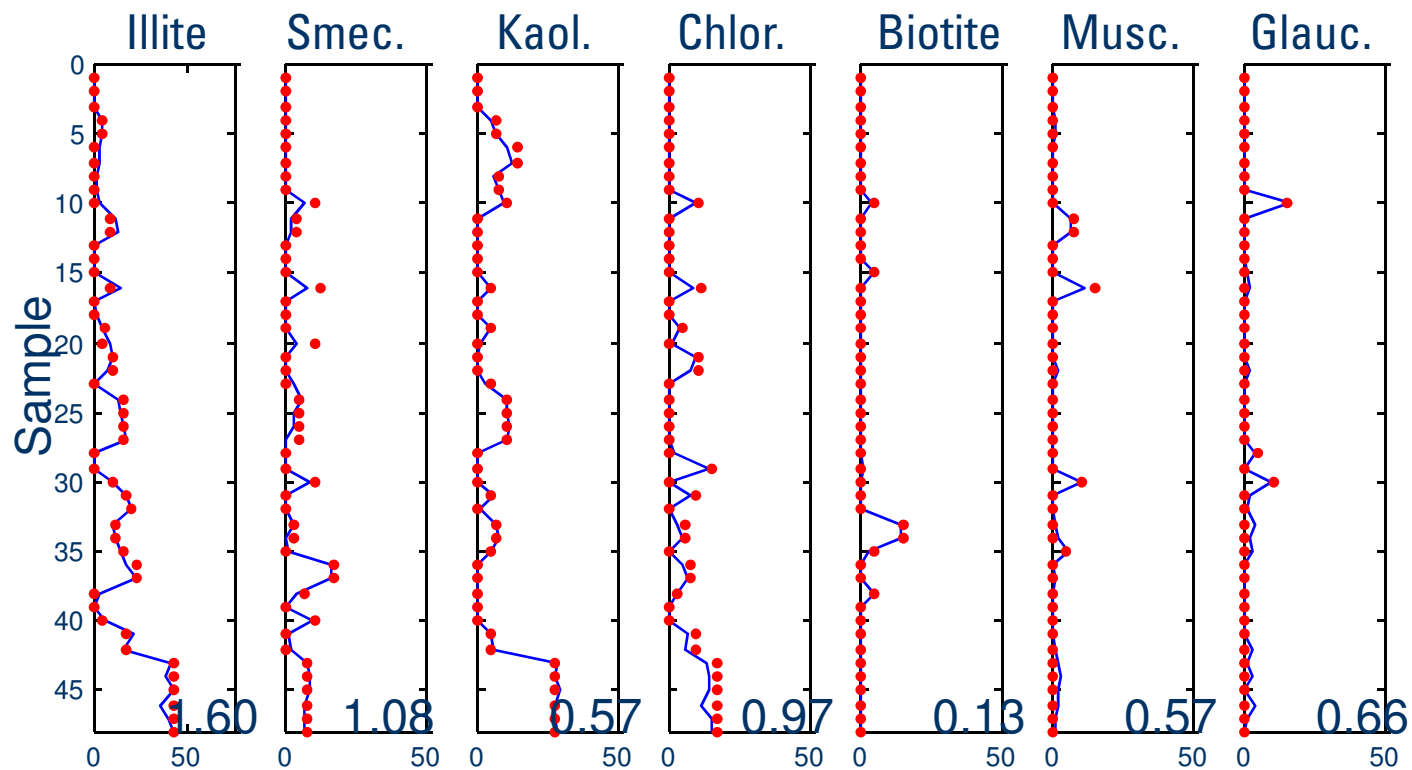


Table 2. Mean and standard deviation of selected elements in the mineral standards. Included are those elements detectable by current geochemical techniques plus Na and B which may exert an additional perturbation on geochemical or other nuclear logging measurements

Mineral (No. samples)	Si (%)	Al (%)	Fe (%)	Ca (%)	Mg (%)	K (%)	Na (%)	Ti (%)	S (%)	LOI (%)	H <sub>2</sub> O <sup>+</sup> (%)	Th (ppm)	U (ppm)	Gd (ppm)	B (ppm)
Quartz (2)	46.1 0.4	0.0 0.0	0.0 0.0	0.0 0.1	0.0 0.0	0.0 0.0	0.0 0.0	0.02 0.01	0.01	0.4 0.1	0.2	0 0	0.1 0.1	0 0	0 0
Calcite (25)	0.2 0.1	0.0 0.1	0.1 0.1	39.4 0.6	0.2 0.1	0.0 0.0	0.0 0.0	0.00 0.00	0.05 0.05	43.8 0.3	0.1 0.2	0 0	1.4 1.6	0.5 0.8	0.1 0.4
Dolomite (14)	0.6 0.5	0.1 0.1	0.7 1.3	21.6 0.4	12.3 0.8	0.0 0.0	0.0 0.0	0.01 0.01	0.07 0.10	47.1 1.2	0.1 0.1	0.1 0.3	0.9 1.6	1.3 3.6	5 7
Siderite (2)	0.4 0.4	0.7 0.7	40.0 2.7	0.3 0.1	3.0 3.9	0.0 0.0	0.4 0.5	0.01 0.00	0.04 0.05	32.5 2.5	0.9	0.4 0.5	0.5 0.6	0.5 0.6	0
Na-Plagioclase (3)	30.0 2.0	11.8 1.2	0.1 0.1	2.3 2.0	0.1 0.1	0.5 0.4	7.3 1.4	0.01 0.00	0.01 0.02	0.5 0.2	0.2 0.1	0 0	0 0	0.2 0.4	28 19
Ca-Plagioclase (4)	21.7 1.5	17.7 1.0	0.3 0.1	12.1 1.5	0.3 0.1	0.0 0.0	1.4 1.0	0.02 0.01	0.00 0.00	0.7 0.2	0.3 0.1	0 0	0.1 0.1	0.1 0.1	11 10
K-Feldspar (6)	30.0 0.3	10.0 0.1	0.2 0.2	0.1 0.1	0.0 0.0	10.2 0.6	2.0 0.4	0.01 0.00	0.00 0.00	0.5 0.3	0.4 0.1	1.1 1.1	0.4 0.5	0.3 0.4	21 34
Opal (1)	40.0	1.4	0.5	0.5	0.3	0.5	0.7	0.10	0.35	6.5	4.2	4.7	6.5	1.3	160
Muscovite (2)	21.2 0.6	19.1 0.6	1.3 0.8	0.1 0.1	0.1 0.0	7.8 0.5	0.5 0.1	0.03 0.02	0.04 0.05	4.8 0.1	3.5 1.0	0 0	0.7 0.9	0.0	450 260
Biotite (1)	18.2	6.0	13.6	0.2	7.7	7.2	0.4	1.48	0.07	0.8	1.1	1.5	0.7	0.2	35
Kaolinite (9)	20.8 0.4	20.4 0.5	0.4 0.3	0.1 0.1	0.1 0.1	0.1 0.1	0.1 0.1	1.13 0.21	0.01 0.01	14.2 0.3	12.9 0.8	19 6	3.2 0.5	4 2	14 5
Illite (6)	24.9 1.8	10.5 0.8	4.8 0.9	0.5 0.5	1.2 0.3	4.5 1.0	0.4 0.2	0.50 0.07	0.6 0.5	9.9 2.1	5.5 0.6	12 2	4.8 4.6	4 2	163 47
Glauconite (1)	23.1	4.4	15.5	0.5	2.1	5.9	0.0	0.09	0.1	8.3	6.1	3	5.4	4	500
Smectite (8)	26.4 1.6	9.1 0.9	2.0 1.5	1.3 0.5	2.2 0.9	0.6 0.8	0.7 0.6	0.15 0.10	0.02 0.03	16.1 4.7	5.8 1.4	26 7	7.1 6.3	8 2	21 16
Chlorite, all (5)	14.0 3.5	9.6 0.8	20.8 5.5	0.7 0.9	4.8 3.4	0.4 0.5	0.1 0.2	1.32 1.06	0.1 0.1	8.8 2.0	9.2 2.1	7 8	2.9 2.2	5 5	20 25
Chlorite, Sed. (2)	17.9 0.3	9.0 0.8	16.4 0.2	1.6 0.8	2.5 0.1	0.9 0.2	0.3 0.1	2.37 0.30	0.2 0.2	8.1 0.8	7.0 0.3	16 1	4.2 0.5	10 0.3	47 3



Table 3. Mean and standard deviation of  $\gamma$ -ray,  $\Sigma$ , and the  $P_e$  of the standard mineral samples. Also shown are the values of  $\Sigma$  and the values of  $p_e$  obtained using the chemical formula (Ellis *et al.*, 1988)

Mineral (No. samples)	Computed $GR_{mat}$ (API)	Computed $\Sigma_{mat}$ (cu)	Formula $\Sigma_{mat}^*$ (cu)	Computed $P_e$ (peu)	Formula $P_e^*$ (peu)
Kaolinite (9)	104 22	20.1 2.1	13.04	2.1 0.2	1.49
Illite (6)	160 37	40.6 5.6	16.74	4.0 0.2	3.03
Smectite (8)	168 71	20.0 2.3	8.34‡	2.9 0.4	1.63‡
Chlorite, all (5)	56 53	43.7 7.8	47.44§	8.1 1.2	12.36§
Chlorite, Sed. (2)	111 13	50.5 0.8	47.44§	7.8 0.1	12.36§
Glaucosite (1)	150	89.6	20.89	6.7	4.79
Muscovite (2)	130 0	95.3 38.7	17.06	4.0 1.1	2.40
Biotite (1)	127	54.1	35.09	7.0	8.70
K-Feldspar (6)	171 7	15.3 2.8	15.82	3.4 0.6	2.86
Na-Plagioclase (3)	8 6	11.4 2.5	7.64	2.1 0.2	1.68
Ca-Plagioclase (4)	1 1	9.4 1.2	7.38	3.0 0.2	3.13
Quartz (2)	1 1	4.7 0.1	4.55	1.9 0.0	1.81
Opal (1)	79	22.6	5.26	2.5	1.75
Calcite (25)	11 13	7.4 2.1	7.08	5.2 0.4	5.08
Dolomite (14)	8 13	6.9 3.3	4.7	3.4 0.4	3.14
Siderite (2)	6 8	54.2 8.9	52.78	18.6 9.5	14.69

\* Ellis *et al.* (1988).

† Peu = barns/electron.

‡ Montmorillonite—no interlayer water.

§ Fe-chlorite.

Table 4. Mean and standard deviation of thermal neutron porosity (TNPH) and epithermal (ENPH) neutron porosities of the mineral standard samples. Also shown are the values calculated by Ellis *et al.* (1988) from mineral formulae

Mineral (No. samples)	Computed TNPH* (ls units)§	Formula TNPH† (ls units)	Computed ENPH‡ (ls units)	Formula ENPH† (ls units)
Kaolinite (9)	45.0 3.2	45.1	43.3 2.9	47.8
Illite (6)	24.7 2.8	15.8	17.6 2.6	12.7
Smectite (8)	21.8 6.0	11.5¶	17.8 6.1	12.6¶
Chlorite, all (5)	>48.2	>60**	61.0 17.6	>60**
Chlorite, Sed. (2)	>48.2	>60**	42.9 1.8	>60**
Glaucanite (1)	—††	17.5	20.2	13.2
Muscovite (2)	>20.8	16.5	10.7 3.2	13.4
Biotite (1)	11	15.5	5.2	13.1
K-Feldspar (6)	-0.6 0.6	-1.1	-1.0 0.3	-1.5
Na-Plagioclase (3)	-0.5 0.5	-1.3	-0.8 0.2	-1.0
Ca-Plagioclase (4)	-0.8 0.4	-1.6	-0.7 0.4	-1.3
Quartz (2)	-1.8 0.3	-2.1	-0.8 0.4	-1.1
Opal (1)	8.5	1.9	4.7	3.3
Calcite (25)	0.2 0.3	0.0	0.0 0.2	0.0
Dolomite (14)	1.5 1.1	0.5	1.7 0.3	1.7
Siderite (2)	18.4 7.3	12.9	11.1 6.5	6.3

\* Thermal neutron porosity.

† Ellis *et al.* (1988).

‡ Epithermal neutron porosity.

§ Limestone equivalent units.

¶ Montmorillonite—no interlayer water.

\*\* Fe-chlorite.

†† High level of thermal neutron absorbers render calculation meaningless.

Table A2

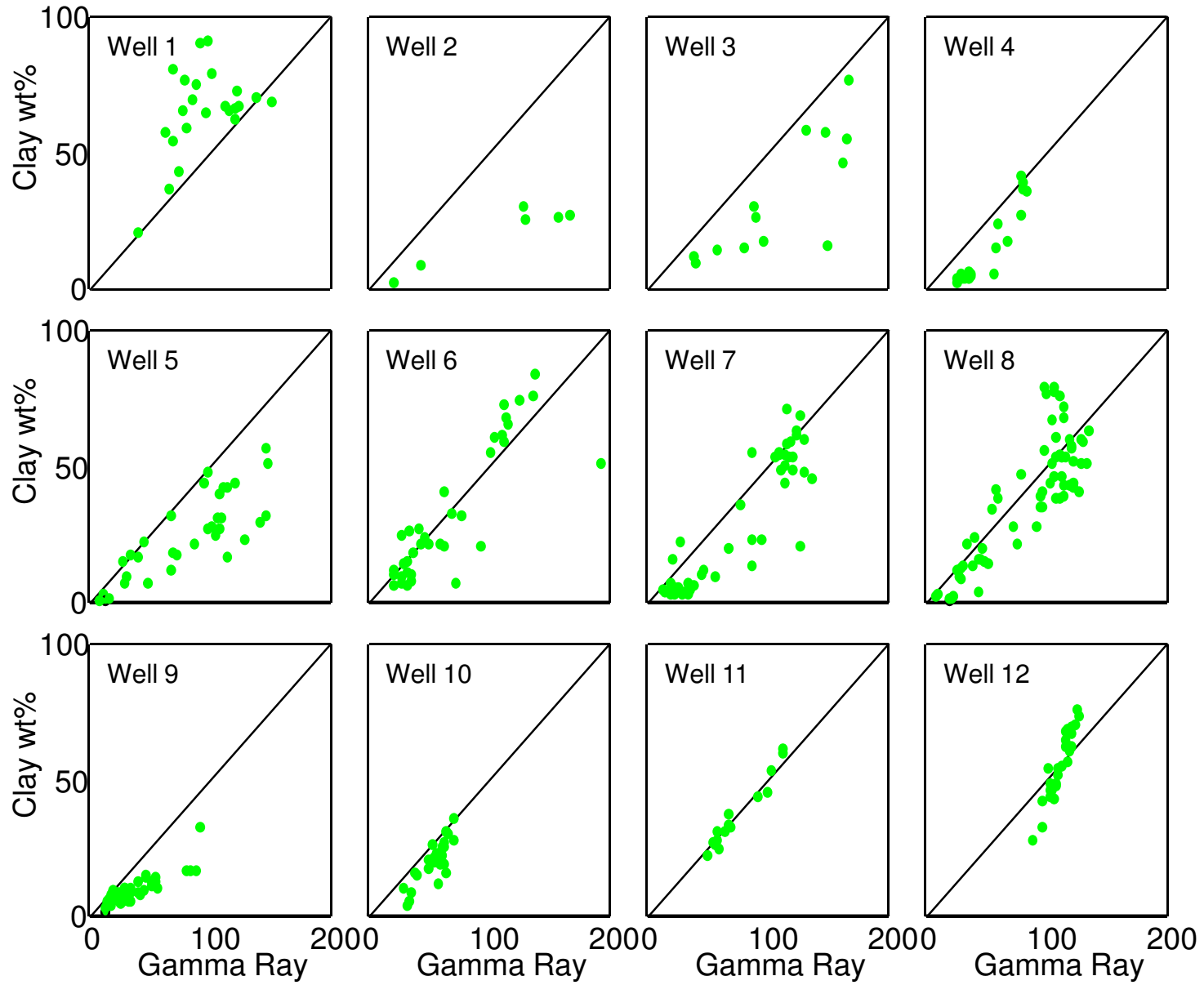
Standard	Li	B	V	Zr	Hf	Th	U	Be	Sc	Cr	Mn	Co	Ni	Cu	Zn	Ga	As	Se	Rb	Sr
	Concentrations in ppm																			
<i>Kaolinite</i>																				
Kao-1	0	14	170	283	10	23	2.7	1	15.5	98	24	2	23	11.8	12	44.9	1.4	0	3	41
Kao-2	40	20	190	282	8.4	21	4.2	3	27.4	110	0	0	17	10.3	33.6	46.6	4.8	1.8	12	39
Kao-3	140	16	94		9	26	2.7	2	14	86	26	11	36	15	28	50	0	0	20	25
Kao-4	0	9.1	220	290	9	21	2.6	1	15	84	6	5	20	10	16	51	2	0	10	40
Kao-5	88	15	130	190	7	12	3.5	2	17	78	10	12	33	12	50	71.8	2	0.5	10	55
Kao-6	92	14	140	193	7	12	3.7	2	17	92	14	12	44	15	62	72.5	4	0.5	12	74
Kao-7	14	22	83	441	11	21	3.3	1	22.5	190	0	21	20	14.8	42.6	41.5	1.4	0	4	60
Kao-8	21	7.7	205	150	4.6	26	3	2	24.1	110	0	14	1	3.2	3.9	50.8	0.9	0	0	5
Kao-9	54	8.9	116	241	7	12	3.5	2	17.1	83	0	29	30	31.1	42.2	64.5	0.9	0	0	134
Average	49.9	14.1	150	259	8.1	19.3	3.2	1.8	19	103	8.9	11.8	24.9	13.7	32	55	1.9	0.3	7.9	53
Std dev	48.2	4.9	49	90	1.9	5.8	0.5	0.7	5	34	10.4	9.1	12.6	7.5	19	12	1.5	0.6	6.6	36
<i>Illite</i>																				
Ill-1	22	134	150	165	5.5	12	4	5	17.2	110	89	14	36	46.9	159	27.4	58	0.6	211	205
Ill-2	30	190	1000	147	5	14	14.1	6	19	350	94	17	130	80	100	27.4	23	23	195	933
Ill-3	32	120	150	160	5	12	2.5	7	19	98	620	25	63	55	190	27.8	20	0.5	220	108
Ill-4	40	164	176	132	3.5	9.8	2.3	8	19.3	130	137	16	30	43	218	34	37	0	247	141
Ill-5	36	127	148	177	4.3	12	3.5	5	16.5	100	142	17	29	42.4	177	27.5	52	0	207	176
Ill-6	29	242	126	86	3.4	14	2.4	8	17.8	140	121	23	52	17	76.1	33.4	3.1	0	294	274
Average	32	163	292	145	4.5	12.3	4.8	6.5	18	155	201	18.7	56.7	47.4	153	29.6	32.2	4.0	229	306
Std dev	6	47	347	33	0.9	1.6	4.6	1.4	1	87	207	4.3	38.3	20.4	55	3.2	20.8	9.3	36	312
<i>Smectite</i>																				
Sme-1	9	17	10	148	6.9	34	16.3	3	6.84	4	84	2	3	3.2	76.9	26.9	0.5	0	21	409
Sme-2	9	44	120		4	13	2.6	4	13	10	72	13	7	15	42	25	6.1	0	130	360
Sme-3	45	5.7	32		9	25	1.6	4	6	0	1162	4	6	1.5	79	19	0.8	0	20	90
Sme-4	190	7.4	86		8	25	1.5	4	4	0	774	4	6	1.5	68	21	5.6	0	21	377
Sme-5	24	28	10	190	10	31	11.1	3	6	0	30	30	2	4.5	150	32.1	7.3	0	14	251
Sme-6	200	5.7	80	239	8	23	2.3	5	4	0	774	5	2	0	59	22	4	0	16	415
Sme-7	16	18	14	131	6	33	15.3	3	7	0	66	4	1	1.5	69	31.4	2.6	0	26	363
Sme-8	26	45	16	144	6	21	6	3	4	0	56	5	5	2.5	48	18.8	2.6	0	18	148
Average	65	21	46	170	7.2	26	7.1	3.6	6.4	1.8	377	8.4	4.0	3.7	74.0	24.5	3.7	0.0	33.3	302
Std dev	81	16	43	44	1.9	7	6.3	0.7	3.0	3.6	452	9.3	2.3	4.8	33.4	5.2	2.5	0.0	39.3	124
<i>Chlorite</i>																				
mChl-1	6	1.5	290	54	2	0	0	5	52.3	370	687	210	578	34.3	44	37.1	0.6	0	9	2
mChl-2	15	0.5	460		3	1.7	1.1	9	31	100	2943	0	28	12	99	47	0.1	0	4	2
mChl-3	100	2.3	140	10	0	0.6	5.1	7	0	0	5731	0	5	0	530	59	0.8	0	6	7
Chl-1	92	48.7	501	460	10	17	4.5	6	22	630	697	109	126	32.9	244	40.3	7.3	3	47	132
Chl-2	99	44.9	489	237	5.7	15	3.8	6	23.8	550	1400	85	116	22.9	223	36.3	7.1	0	35	137
Average	62	20	376	190	4.1	6.9	2.9	6.6	26	330	2292	80.8	170.6	20	228	44	3.2	0.6	20.2	56
Std dev	48	25	157	205	3.9	8.4	2.2	1.5	19	275	2131	87.4	233.8	15	188	9	3.7	1.3	19.5	72
<i>Sed Chlorite</i>																				
Chl-1	92	48.7	501	460	10	17	4.5	6	22	630	697	109	126	32.9	244	40.3	7.3	3	47	132
Chl-2	99	44.9	489	237	5.7	15	3.8	6	23.8	550	1400	85	116	22.9	223	36.3	7.1	0	35	137
Average	96	47	495	349	7.9	16.0	4.2	6.0	23	590	1049	97.0	121.0	28	234	38	7.2	1.5	41	135
Std dev	5	3	8	158	3.0	1.4	0.5	0.0	1	57	497	17.0	7.1	7	15	3	0.1	2.1	8	4

continued overleaf

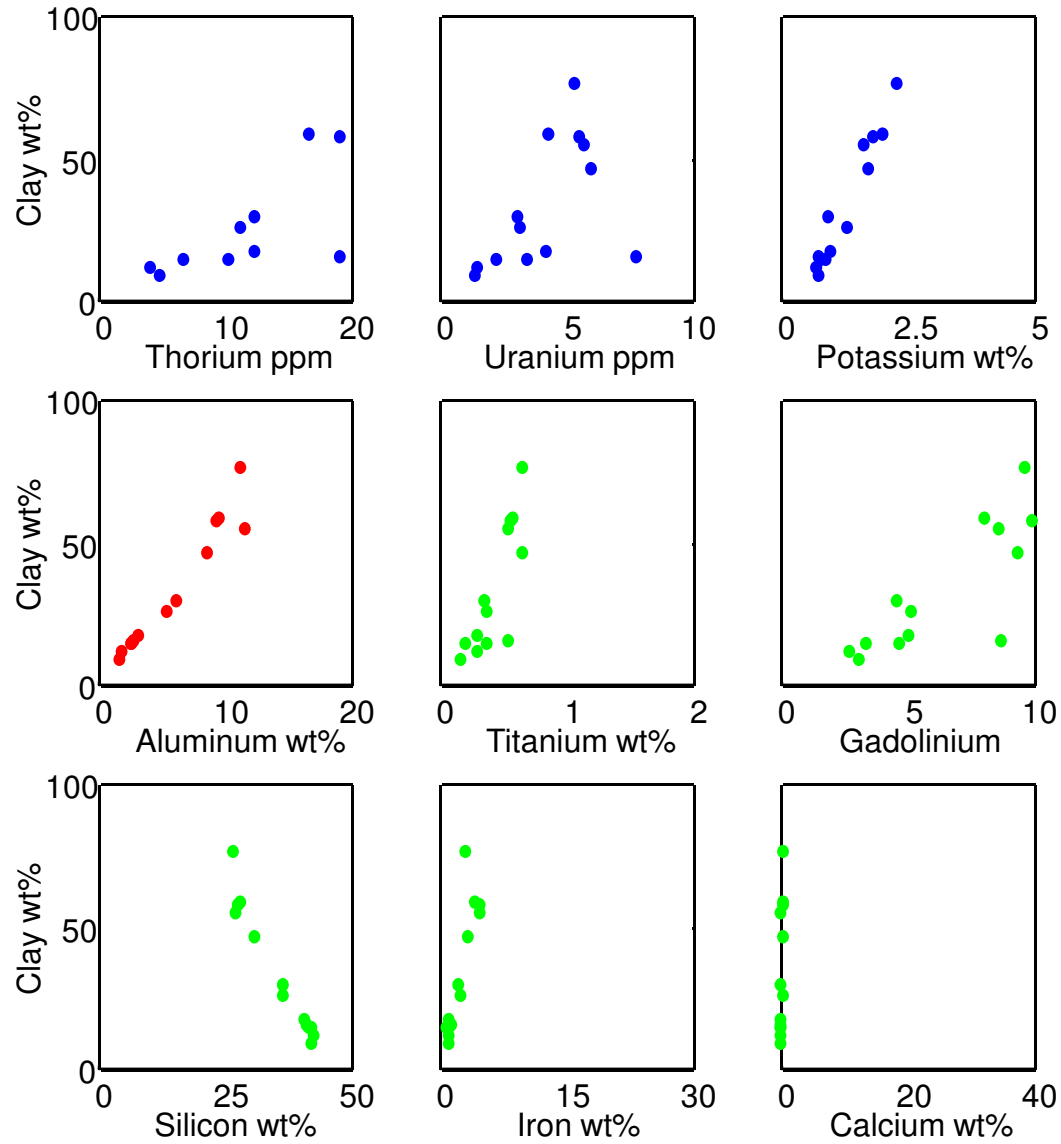
# Development of Applications

- Total clay from chemical data
- Matrix density from chemical data
- More for you to develop

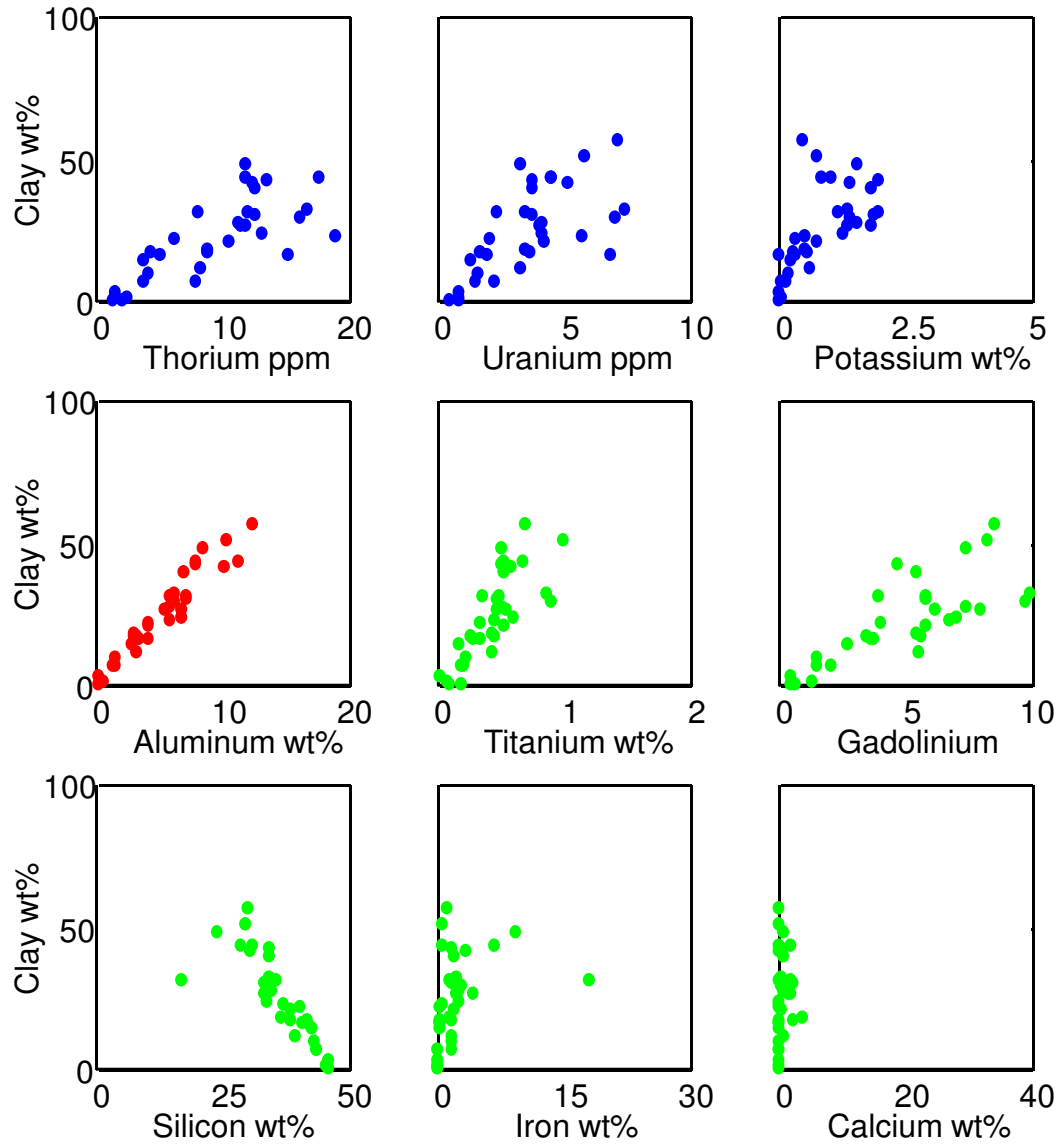
# Clay and Gamma Ray



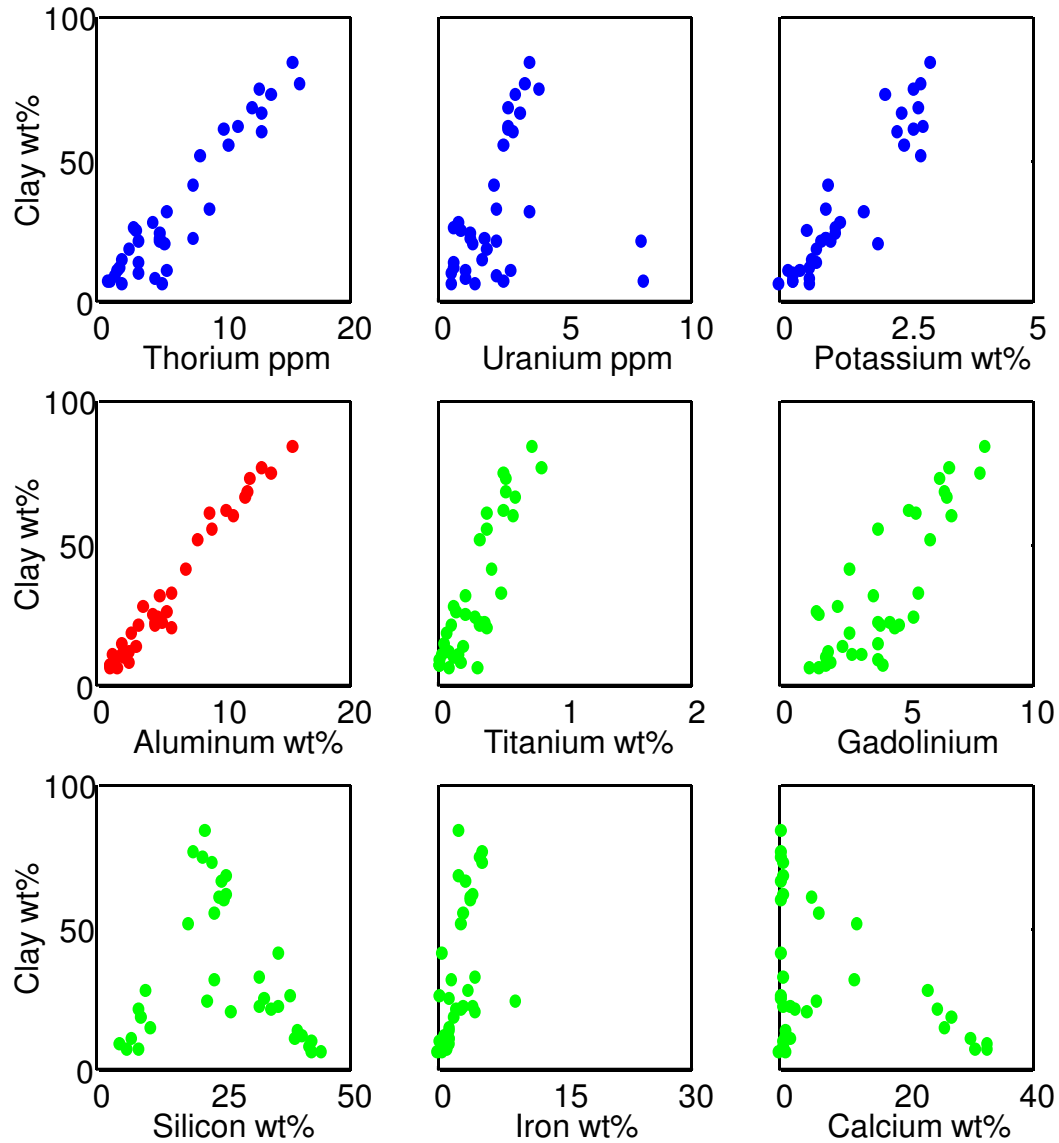
# Clay Elemental Relationships - Well 3



# Clay Elemental Relationships - Well 5

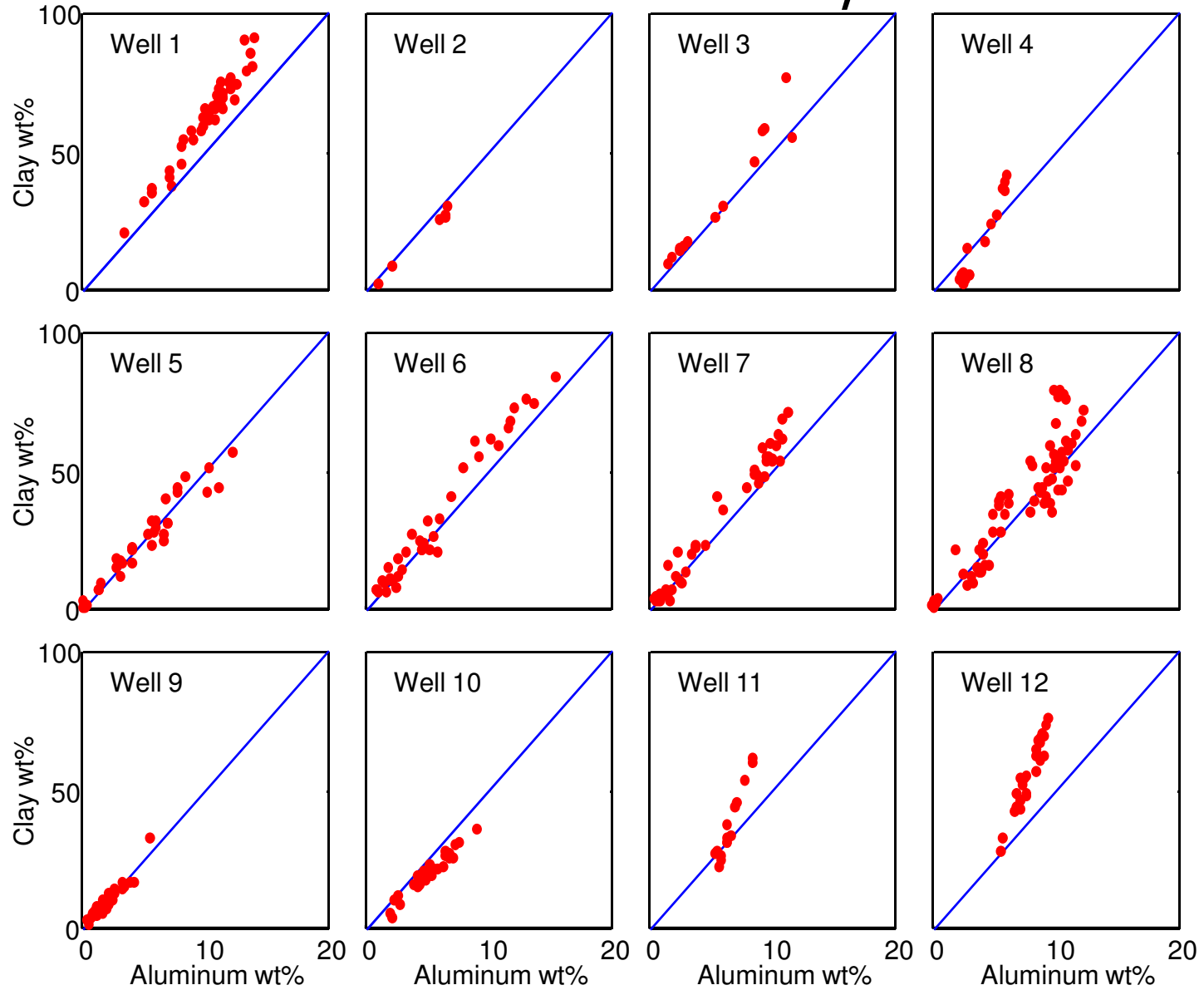


# Clay Elemental Relationships - Well 6

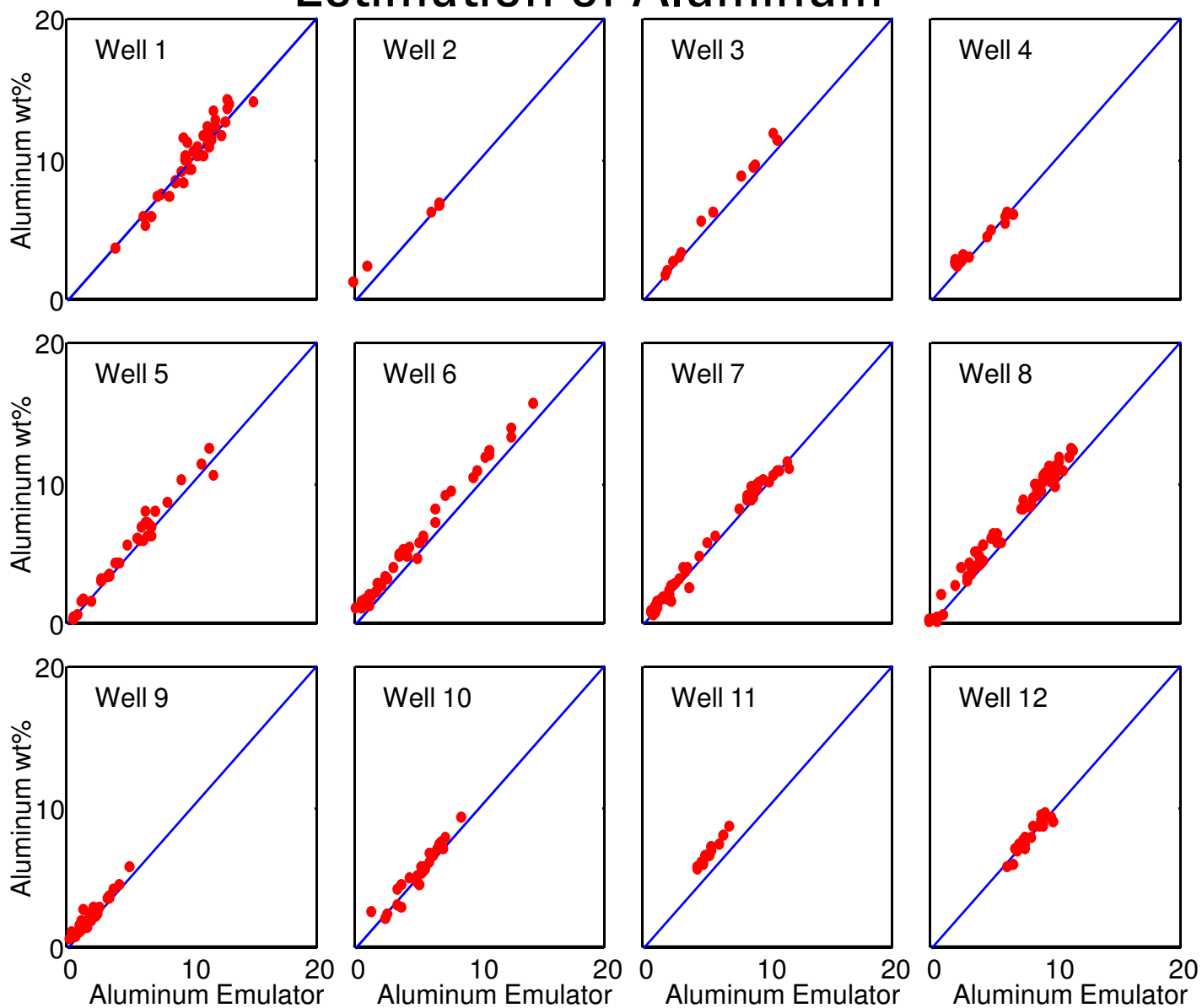




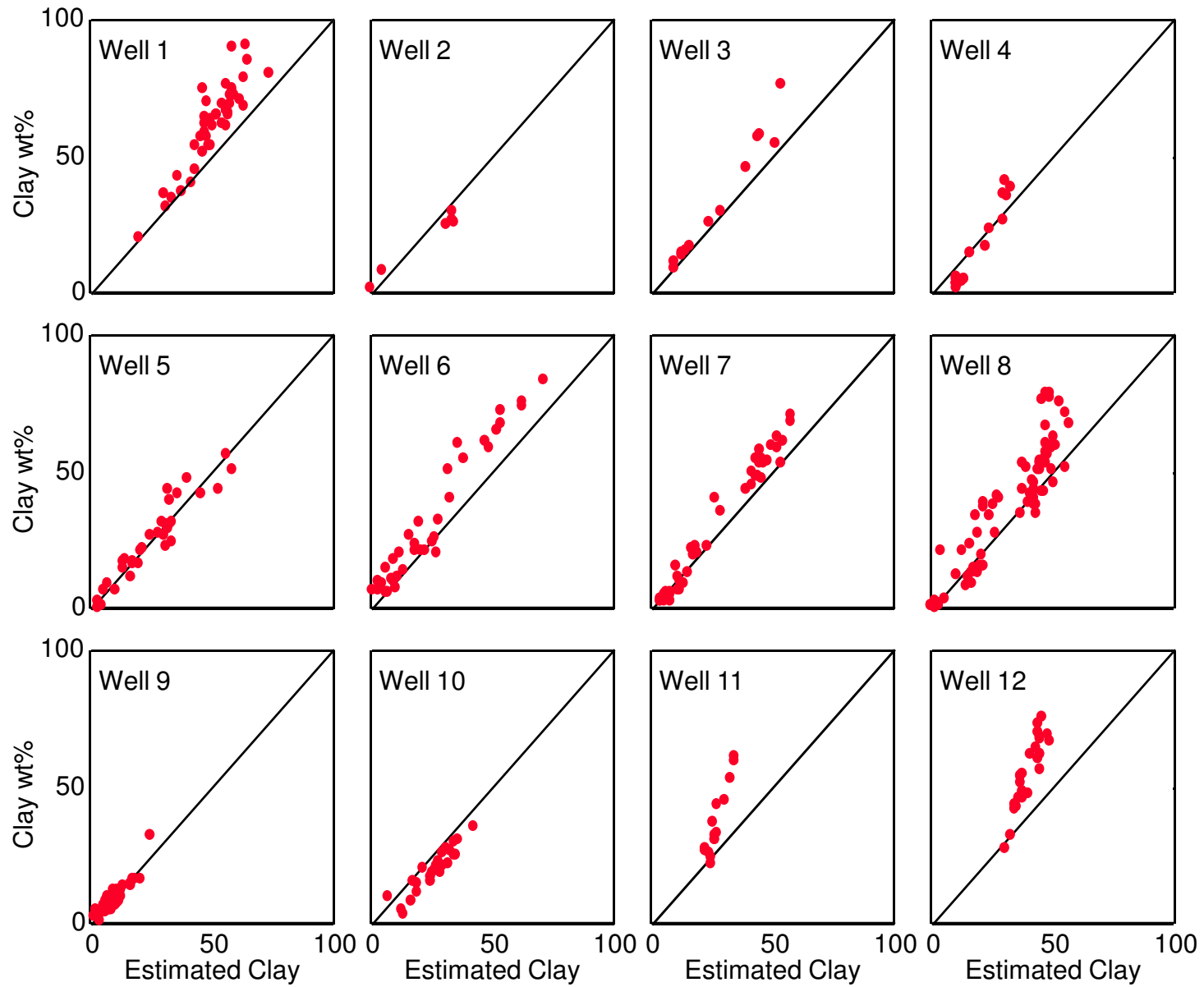
# Aluminum and Clay



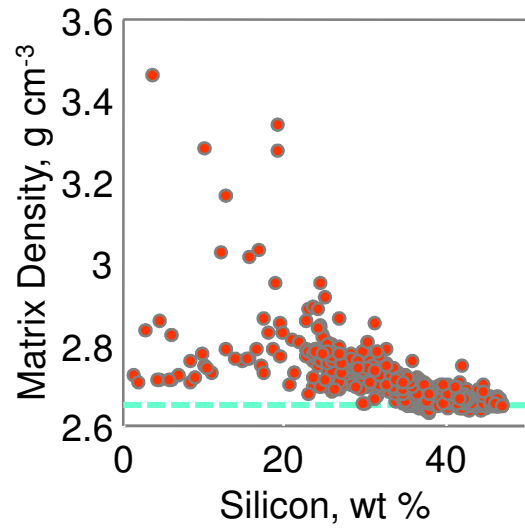
# Estimation of Aluminum



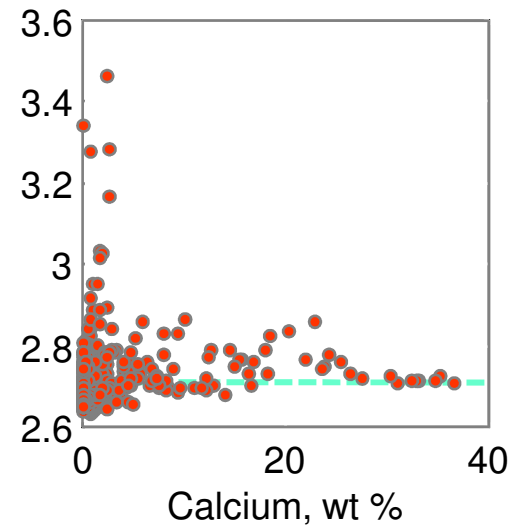
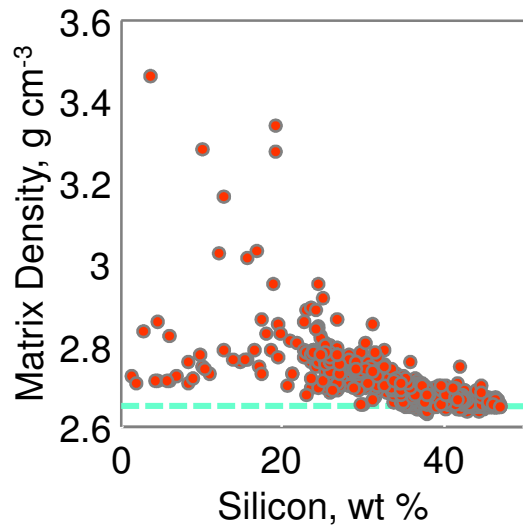
# SpectroLith Clay from Si, Ca, Fe



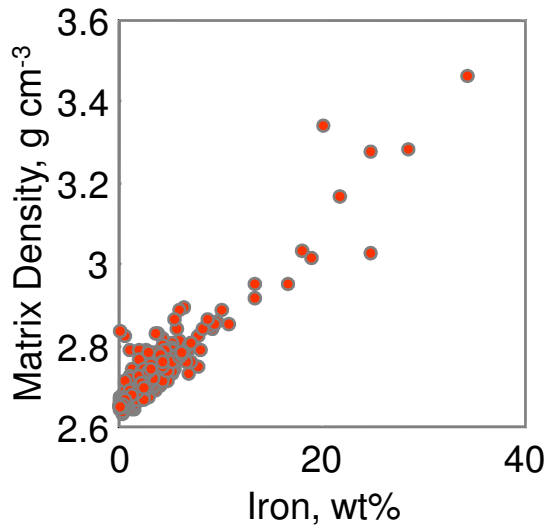
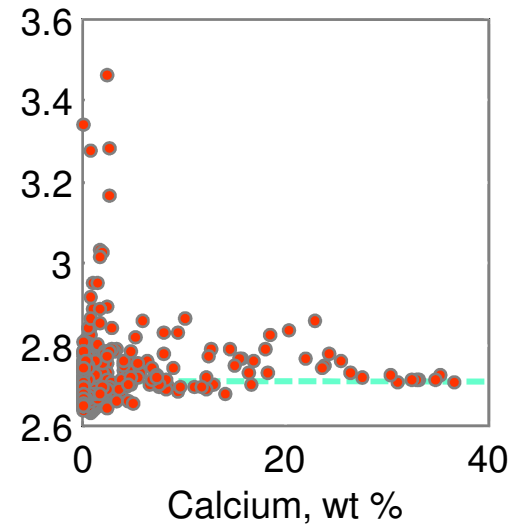
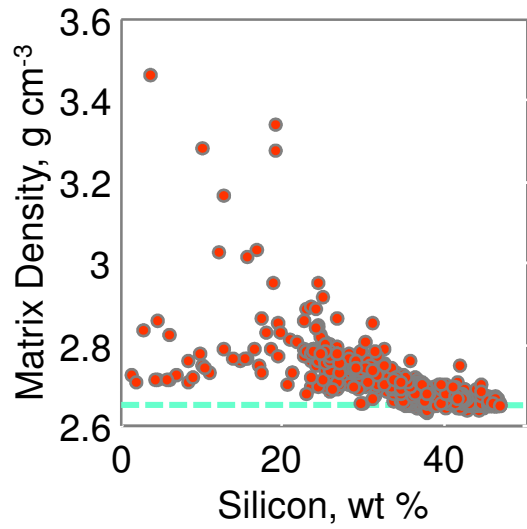
# Changes in $\rho_{ma}$ with Silicon



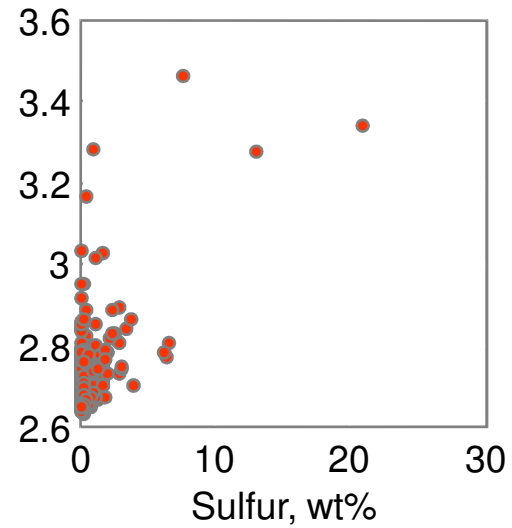
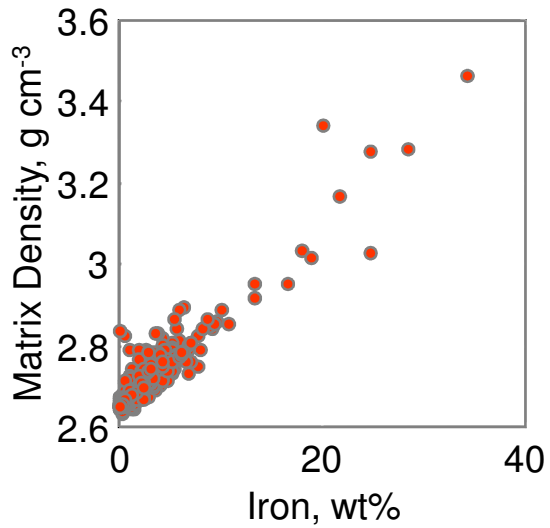
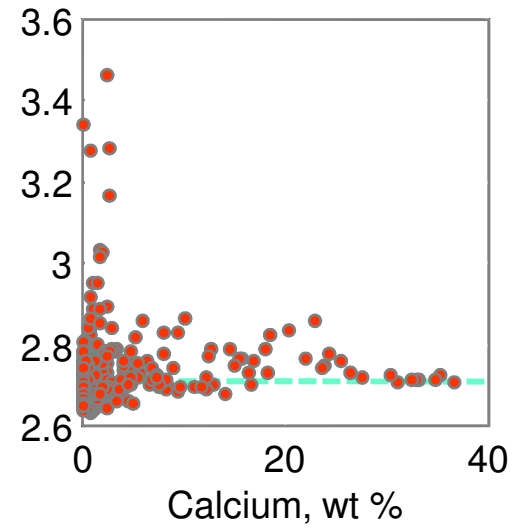
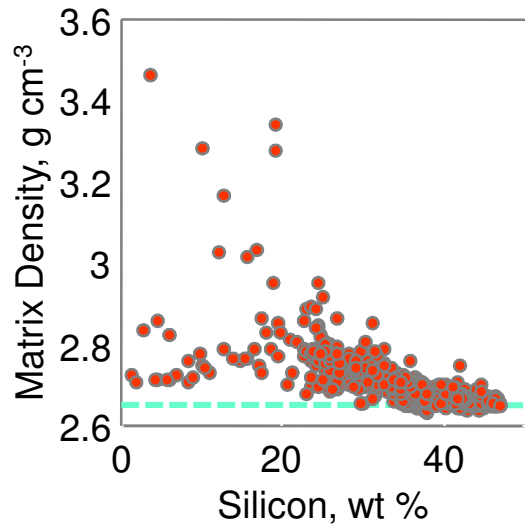
# Variation of $\rho_{ma}$ with Calcium



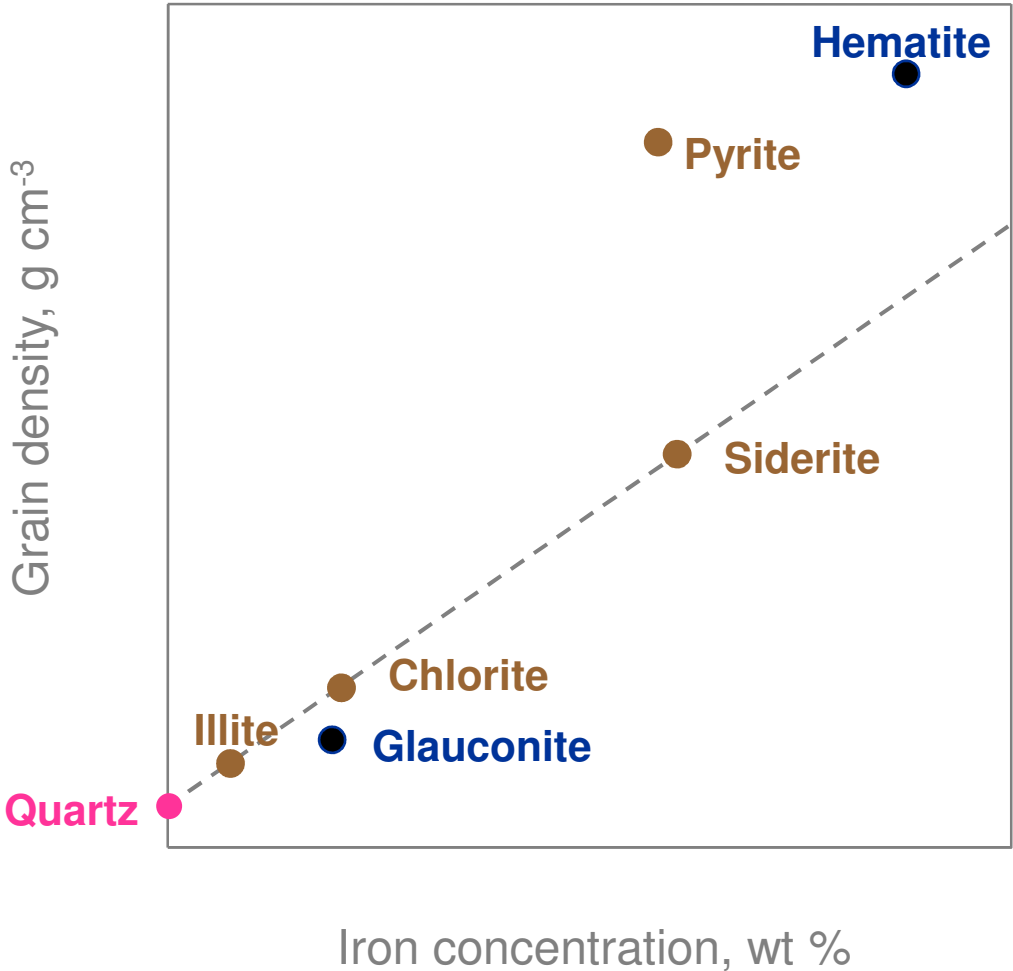
# $\rho_{ma}$ Increases with Iron



# $\rho_{ma}$ Also Increases with Sulfur



# Density of Common Iron-bearing Minerals





# Regression Results

## Non-arkose & Subarkose

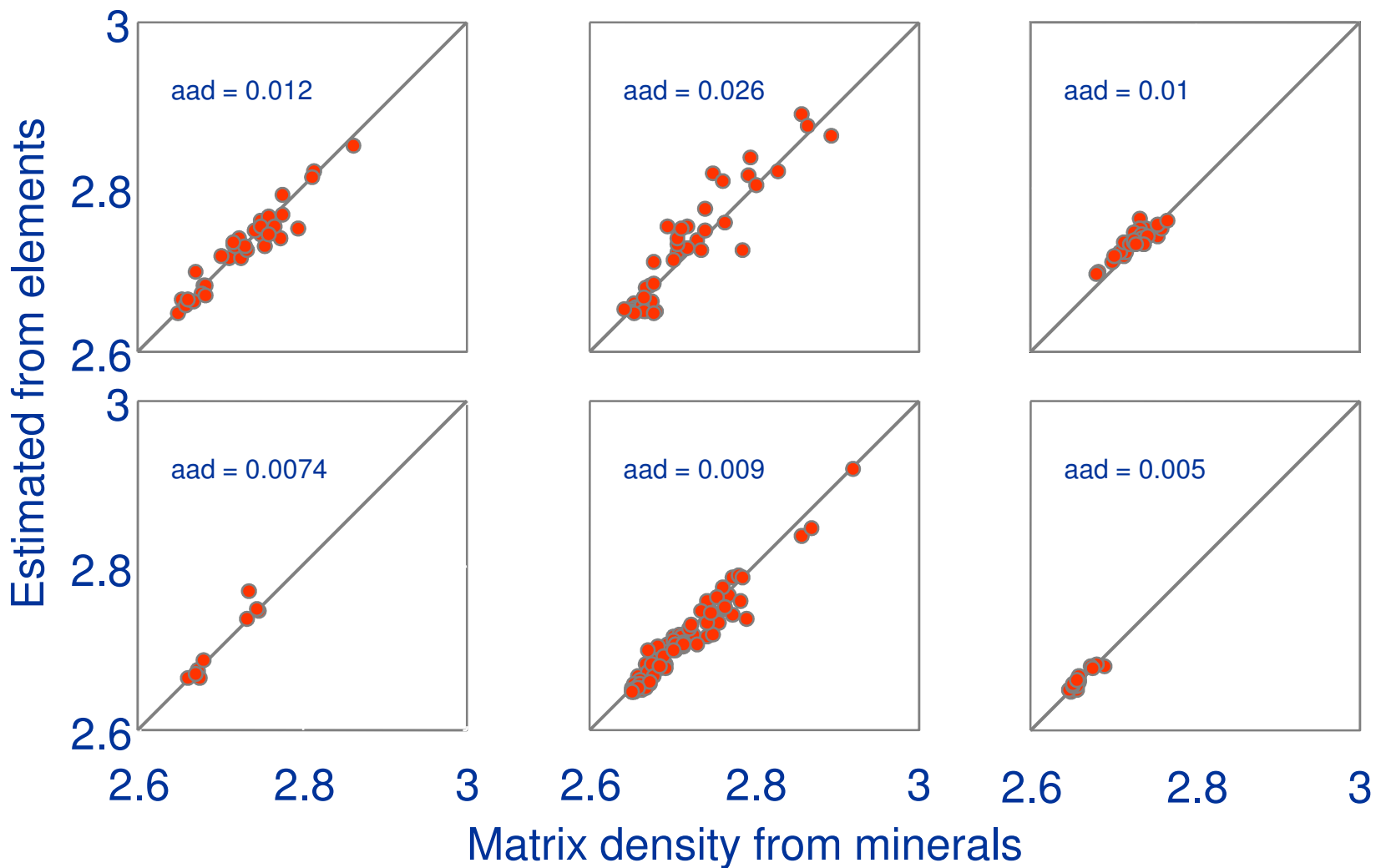
$$\begin{aligned}\rho_{\text{ma}} &= 2.620 \\ &+ 0.0490 \text{ Si} \\ &+ 0.2274 (\text{Ca} + 0.6 \text{ Na}) \\ &+ 1.993 (\text{Fe} + 0.14 \text{ Al}) \\ &+ 1.193 \text{ S}\end{aligned}$$

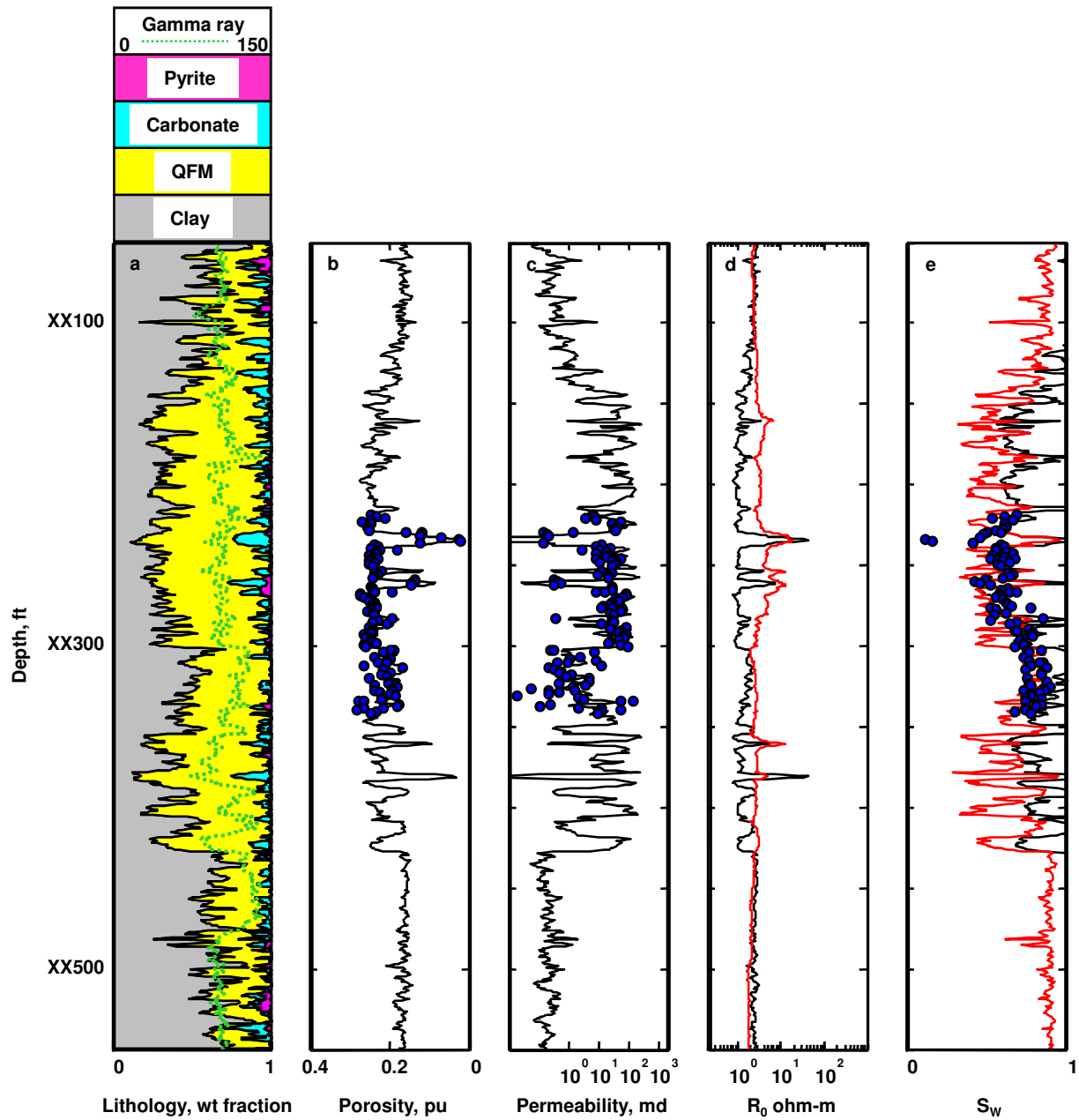
$$r = 0.967; \text{ std error } 0.015 \text{ g cm}^{-3}$$

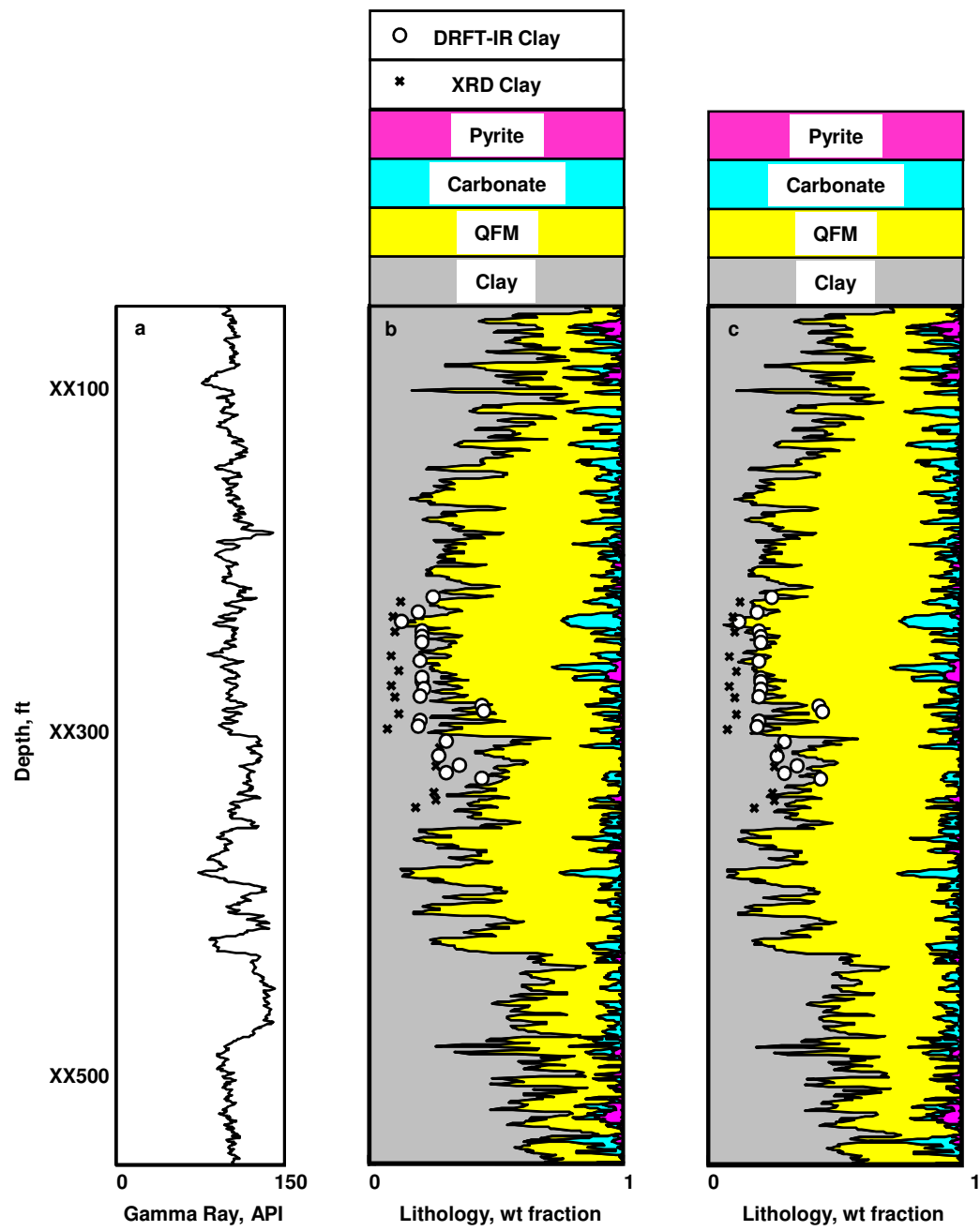
# Measured vs Computed Density

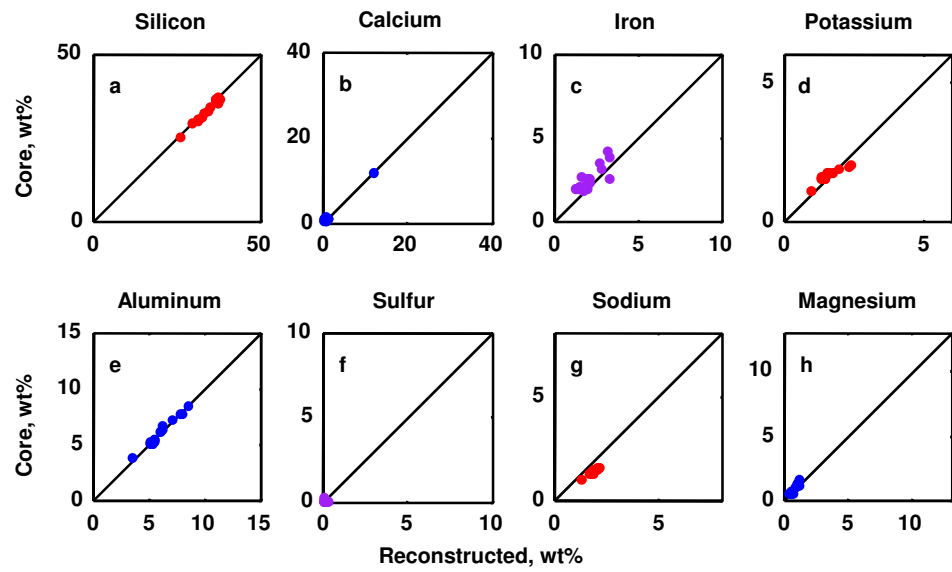
Non-arkose

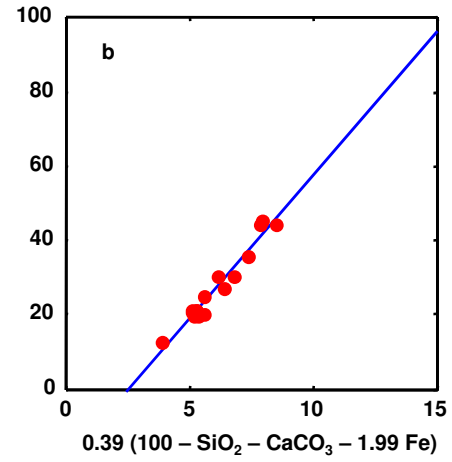
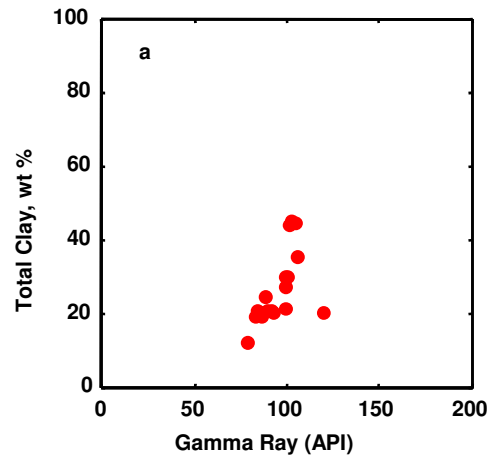
Subarkose

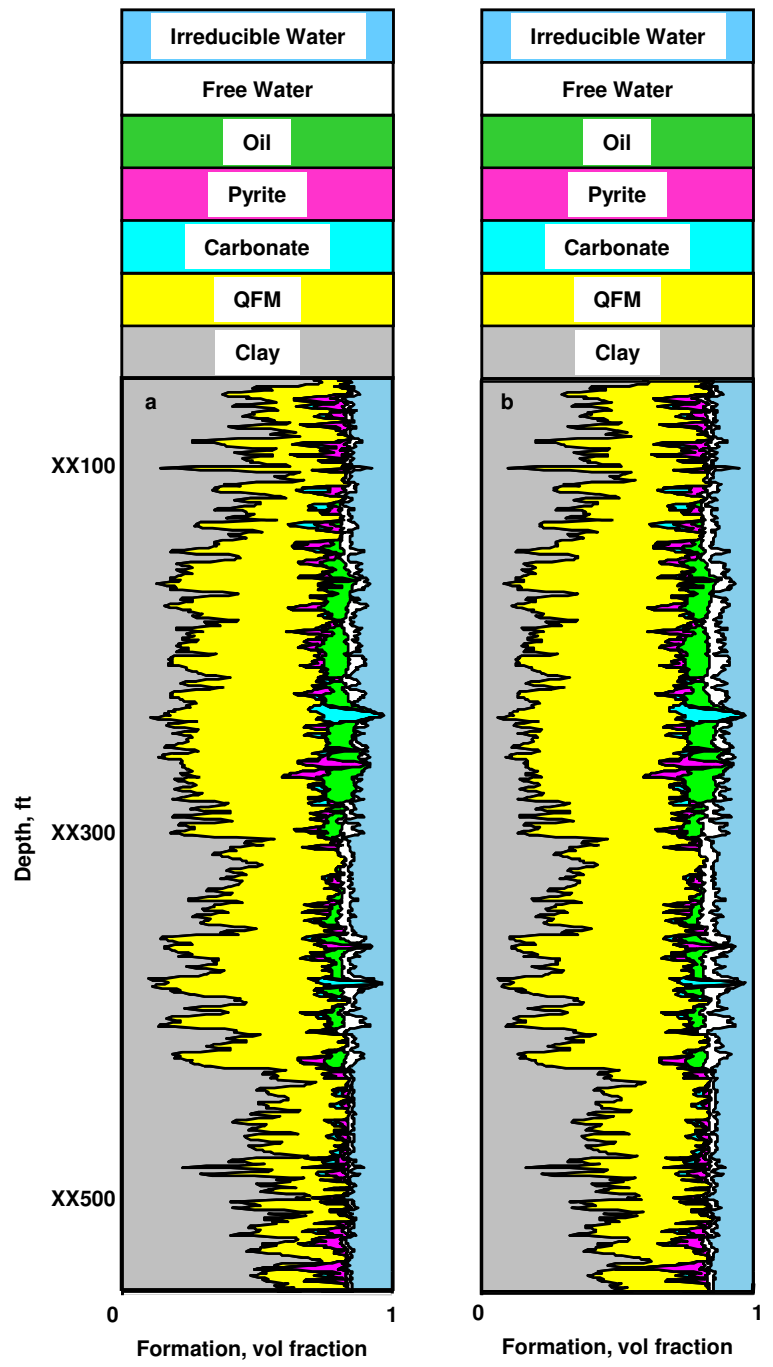




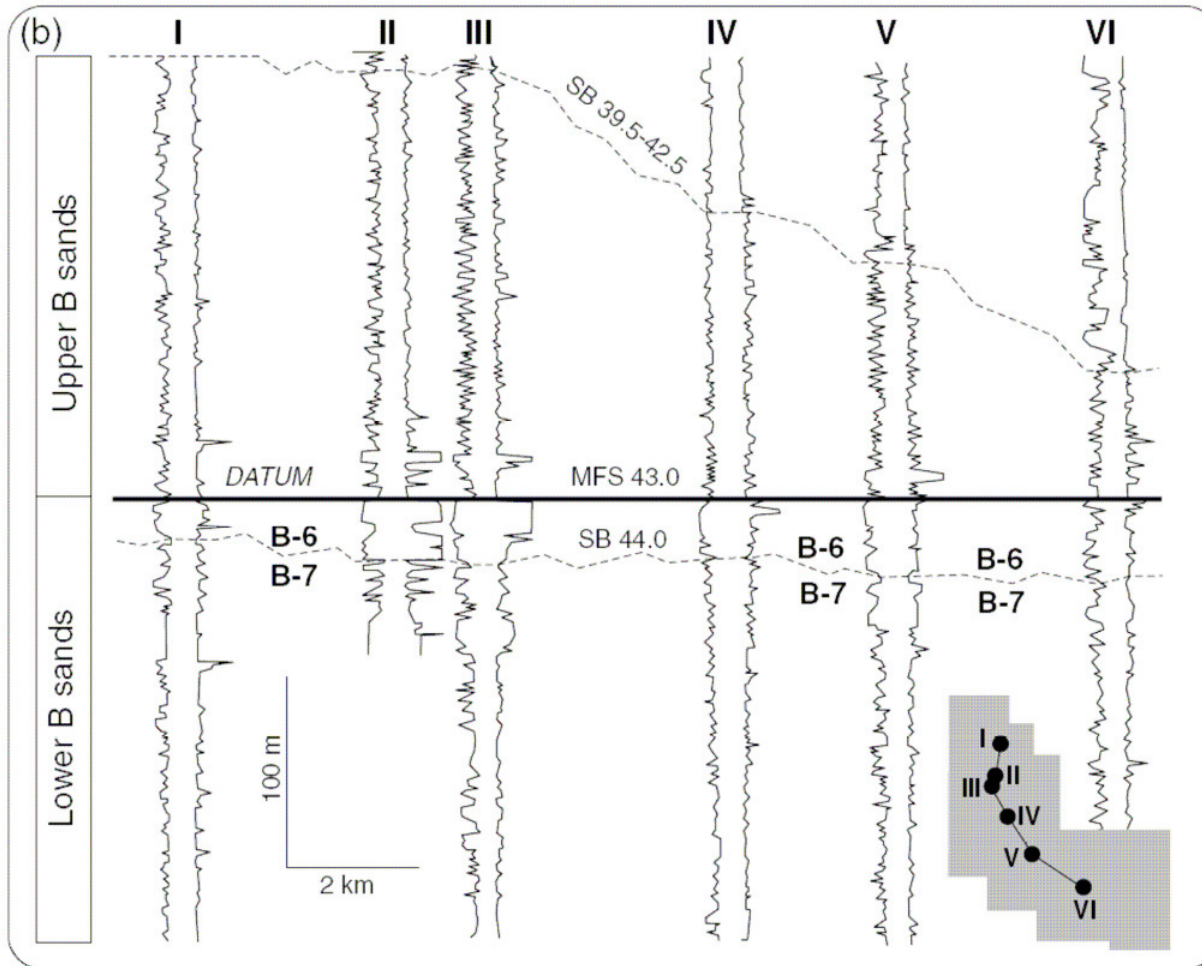








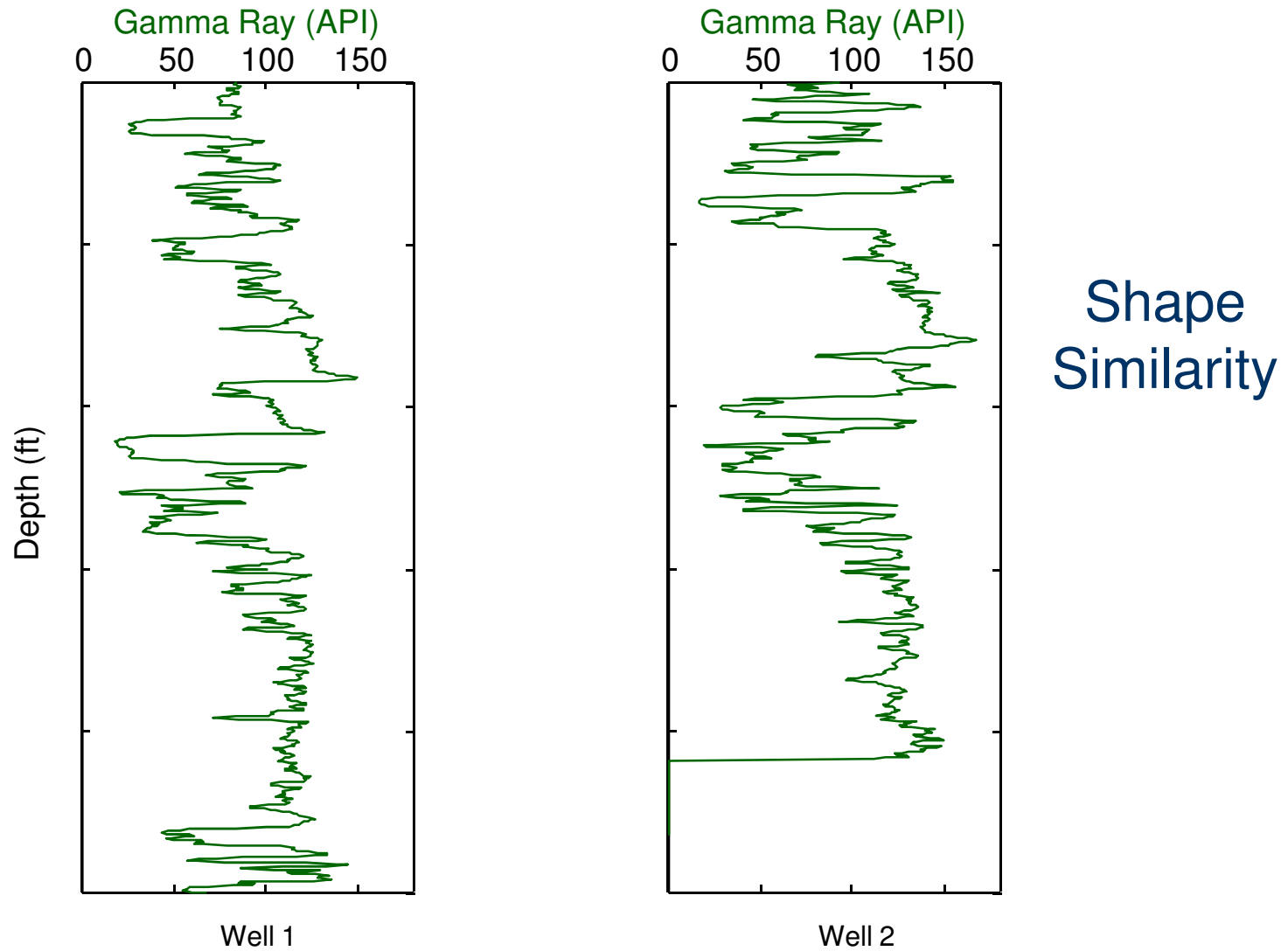
# Well-to-Well Gamma Ray-Resistivity



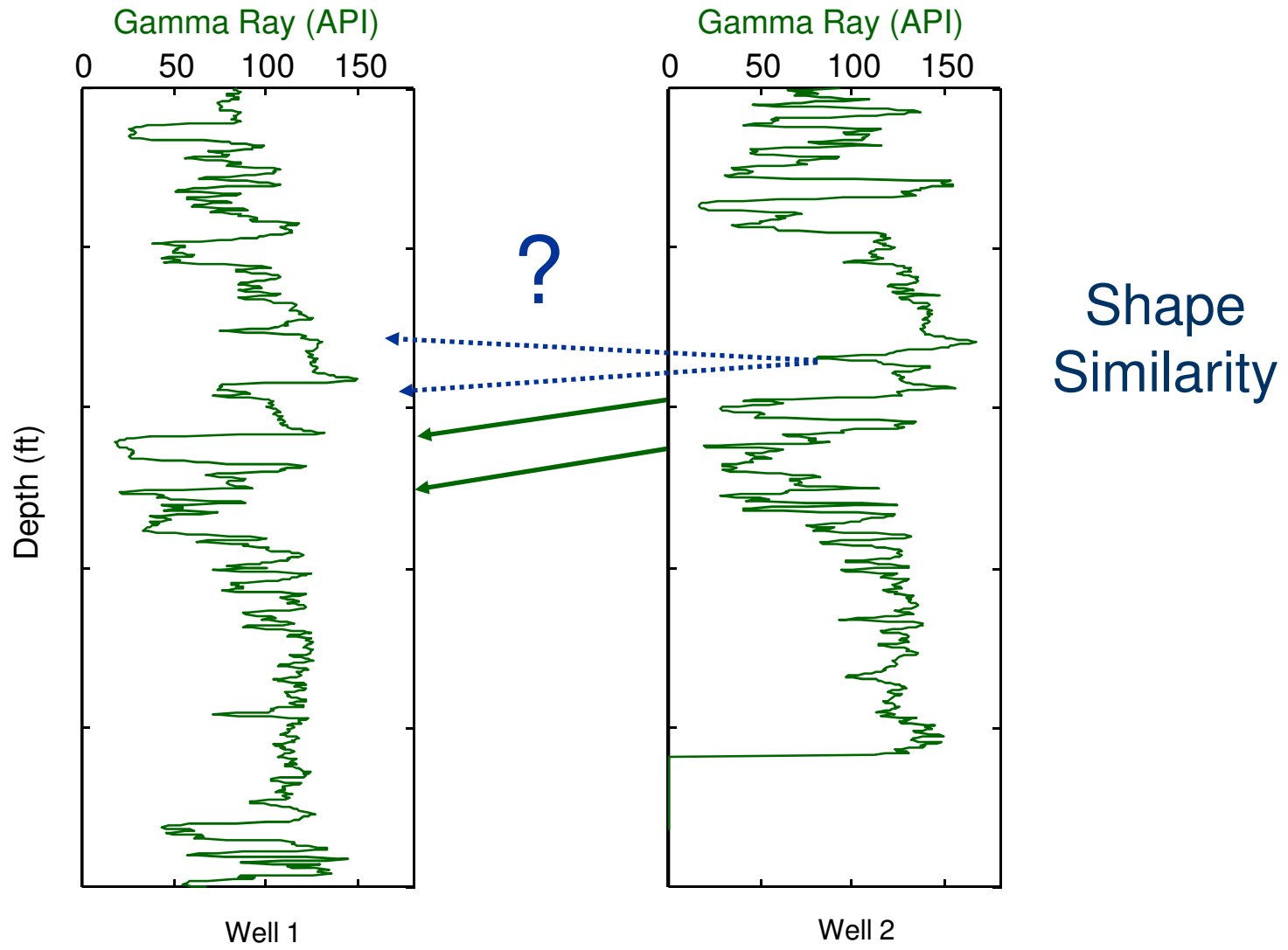
Sometimes these  
Correlations are  
Difficult to understand  
And not repeatable



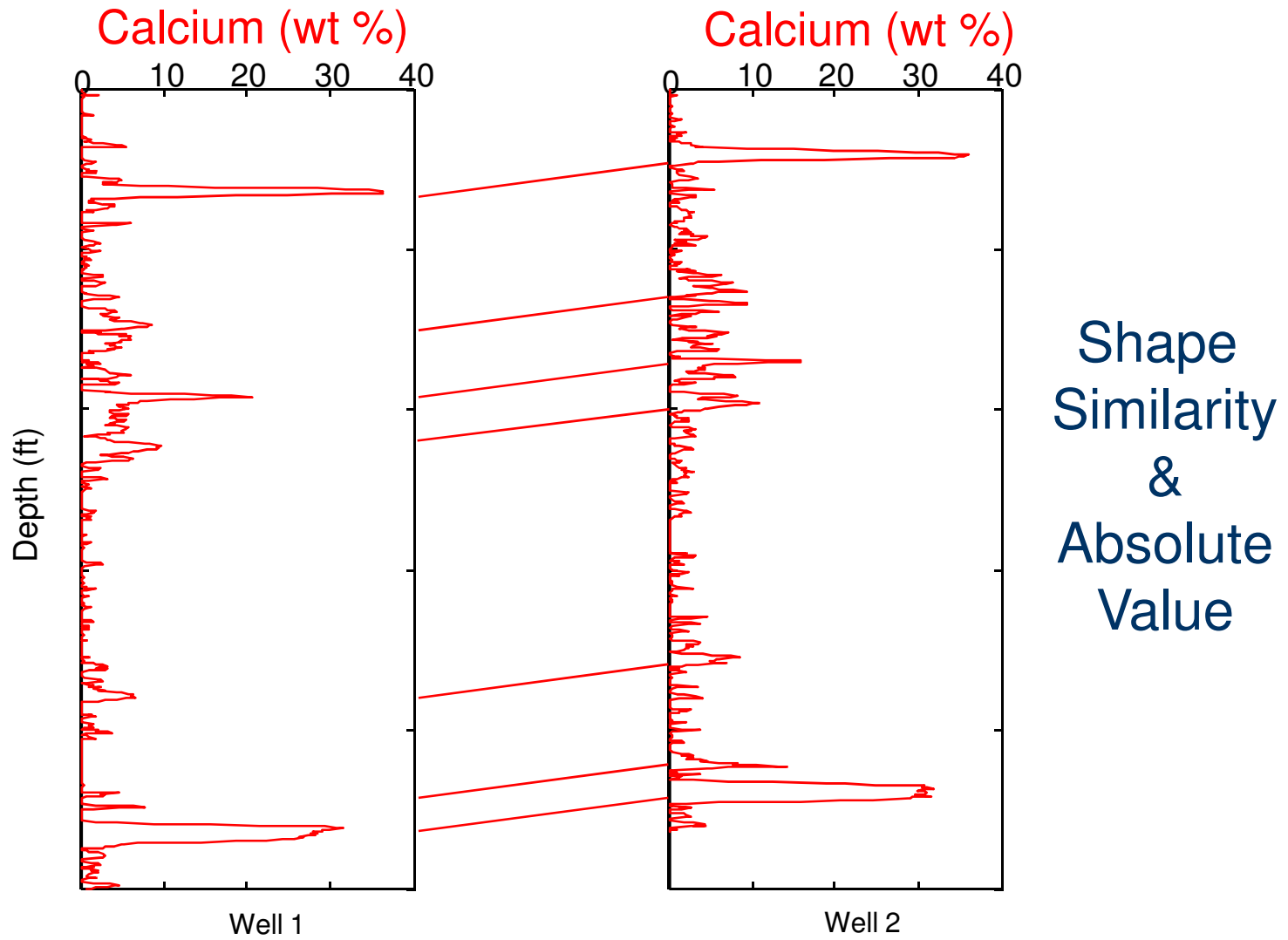
# Ambiguous Correlations with Gamma Ray



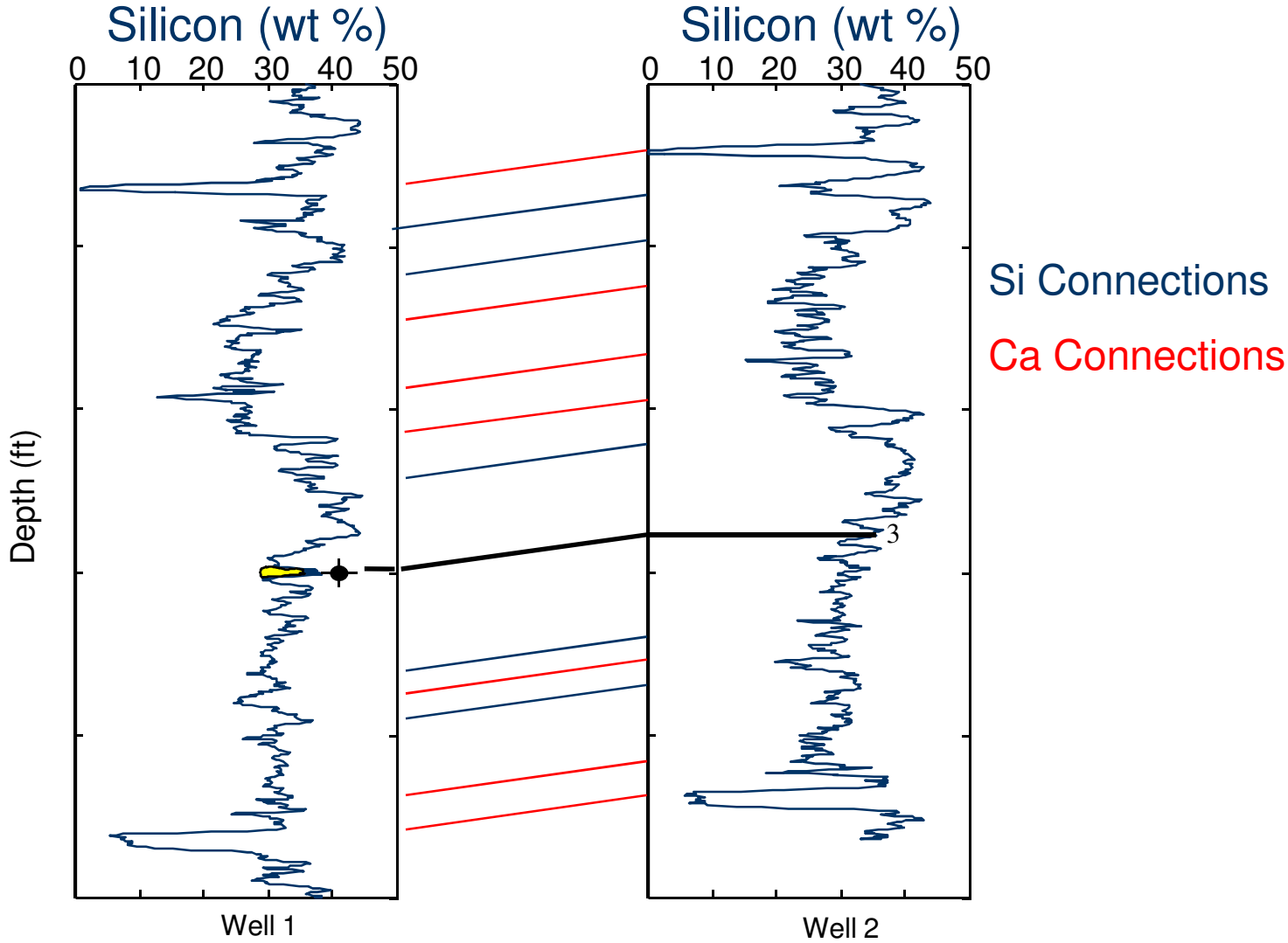
# Ambiguous Correlations with Gamma Ray



# Chemostratigraphy Lowers Ambiguity



# This is the Chemostratigraphy Connection



# Leaps of Science Follow New Analytical Capabilities

- Induced gamma ray spectroscopy is now becoming a standard oilfield service
- More data in an hour than in a lab geochemist's lifetime
- New elements are around the corner
- Challenge is on Academia and Industry to maximize use of these new data



# Scope

## The New Age of Drilling

These new-generation while-drilling services dramatically improve drilling performance and well placement—leading to increased production, sooner. Scope\* services set new standards for reliability and data quality, while quadrupling the data rate over the industry standard of 3 bps.

### EcoScope

EcoScope\* logging while drilling. Delivering industry-first measurements, faster.

- Increases efficiency and safety by integrating drilling and formation evaluation sensors in one collar; eliminates one radioactive source
- Improves well placement with elemental capture, porosity, lithology, density, sigma, and resistivity measurements
- Improves drilling performance with measurements of annular pressure, borehole diameter, and downhole shock
- Logs at speeds of 450 ft/hr while recording 2 points/ft

### StethoScope

StethoScope\* formation pressure while drilling. Improving efficiency and reducing risk.

- Saves time by measuring reservoir pressure in less time than needed to make a connection
- Allows mud weight optimization to avoid kicks and drilling delays
- Eliminates need to orient the tool—even in vertical wells—by using a setting piston
- Improves measurement quality through Smart Pretest\* system and pumps-off option

### TeleScope

TeleScope\* high-speed telemetry while drilling. Transmitting more data, faster.

- Improves efficiency by transmitting data at rotary steerable drilling speeds
- Delivers 4 times the data rate of the industry standard by using the Orion\* telemetry protocol
- Improves well placement by providing comprehensive picture of downhole environment through real-time measurements from multiple tools
- Sets a new standard for data transmission

[www.oilfield.slb.com/scope](http://www.oilfield.slb.com/scope)